AD-A062 033 BOSTON COLL CHESTNUT HILL MASS DEPT OF PHYSICS F/G 4/1
CO-ORDINATED ANALYSIS OF AURORAL DATA ON THE ATS FIELD LINE.(U)
AUG 78 R H EATHER F44620-76-C-0129

UNCLASSIFIED AFOSR-TR-78-1501 NL

| OF |
AD A062033

END
DATE FILMED
3-79
DDC

(4) LEVEL II

(18) AFOSR-TR-78-1501 (19)

(6) CO-ORDINATED ANALYSIS OF AURORAL DATA ON THE ATS FIELD LINE.

(10) Principal Investigator: Robert H. Eather
Physics Department
Boston College
Chestnut Hill, MA 02167

(11) 31 Aug 78

(9) Final Report,
30 Jun 1976 - March (31) 1978

(12) 52 p.

(15) F44620-76-C-0129

Approved for public release. Distribution unlimited.

(16) 2311 (17) A1

This research was supported by the Air Force Office of Scientific Research.

404 606

Introduction

During February - March, 1975, detailed photometric data was obtained along $\pm 5^{o}$ of the geomagnetic meridian centered at the base of the ATS-5 and ATS-6 field lines. DMSP satellite images were also available for the period.

This project was concerned with:

1. Analysis of meridian-scanning photometer data and presentation as gray-scale "keogram" plots.
2. Reduction of ATS-5 and ATS-6 particle data, and presentation as gray-scale electron and proton "spectrograms."
3. Comparison of co-ordinated photometer and DMSP data to absolutely calibrate the DMSP imaging system.
4. Collection of all relevant ground-based magnetograms.
5. Analysis of data to search for relationships between satellite particle fluxes and energy, and auroral intensity at the base of the same field line. In particular, to examine loss-cone fluxes as measured by ATS-6 for this purpose.
6. Publication of results.

Data Analysis

Table 1 gives the dates for which data were analyzed. These were clear, moonless nights for which both ground-based and satellite data were complete.

Table 1

Day	Date (1975)	Keograms	Spectrograms ATS-5	Spectrograms ATS-6	DMSP passes No.	DMSP passes Time(UT)
39	Feb. 8	✓	✓	✓	4665	0557
					4666	0739
40	Feb. 9	✓	✓	✓	4680	0720
43	Feb. 12	✓	✓	✓	4722	0626
					4723	0807
44	Feb. 13	✓	✓	✓	4736	0607
					4737	0747
45	Feb. 14	✓	x	✓	4751	0729
49	Feb. 18	✓	x	✓	4807	0614
					4808	0756
50	Feb. 19	✓	x	✓	4822	0737
64	Mar. 5	✓	x	✓	5020	0642
					5021	0820
66	Mar. 7	✓	x	✓	5049	0744
67	Mar. 8	✓	x	✓	5063	0724
68	Mar. 9	✓	x	✓	5078	0848
71	Mar. 12	✓	x	✓	5120	0753
72	Mar. 13	✓	x	✓	5134	0734
73	Mar. 14	✓	x	✓	5148	0715
74	Mar. 15	✓	x	✓	5162	0659

1. Photometric Data

Analysis of photometric data was a joint computer project between Boston College and Lockheed Research Labs (under subcontract). These

these it was decided that line plots of various satellite measurements (energy flux, mean energy) were necessary. This work is presently in progress.

It is hoped these additional investigations will lead to new publishable results, and that the work will be completed over the next six months. As this contract has expired, this work will be completed at no additional cost. However, it is requested that publication funds that remain unspent in the contract be available for publication charges if an additional publication results.

In addition to the calibration, the nature of particles responsible for the "diffuse aurora" seen on the low-latitude edge of auroral precipitation was investigated. It was found at times the observed intensities could be explained as being due entirely to precipitating protons. At other times, electrons contributed up to 2/3 of the total excitation. We believe this diffuse aurora represents plasma sheet "drizzle," modified at times by particle drifts after substorm rejection events (see Appendix I).

4. Magnetograms

To identify substorm-associated injection events, it is necessary to collect magnetograms from a number of stations well-distributed in longitude. The stations used, and U.T. of local midnight for each, are shown in Fig. 5. From these magnetograms, substorms were identified to aid in interpretation of the relations between keograms and spectrograms.

5. Analysis and Publication

Comparisons of these data have, in general, confirmed results of a similar previous study (R.H. Eather, S.B. Mende, and R.J.R. Judge: Plasma injection at synchronous orbit and spatial and temporal auroral morphology, J. Geophys. Res., 81, 2801, 1976). Expected new insights with this new data set have not materialized. Much of the problem here is that ATS-6 did not sample in the loss cone as was expected when this experiment was planned.

An experimenters meeting was recently held at UCSD (late June, 1978) with Drs. De Forest, McIlwain, Mende, and Eather. It was agreed that it was of little use publishing data that simply confirmed results of the previous study referenced above. However, some events were identified that did not seem to fit the previous picture. To further investigate

tapes had numerous errors and the analysis was more involved and took much more effort and time than expected.

Keograms were prepared at three wavelengths:

a. 4278 N_2^+ - a measure of total energy influx.

b. 6300 OI - a measure of low-energy electron influx.

c. 4861 H_β - a measure of proton influx.

Examples of a quiet day (March 7) and medium-activity day (Feb. 14) are shown as Figs. 1 and 2.

2. Particle Data

Production of particle spectrograms was done under subcontract at University of California, San Diego. Only partial data was available from ATS-5. The greatest disappointment was that the ATS-6 detectors, which were supposed to sample the particle loss cone, were always at higher pitch angles. Consequently one of the major thrusts of this project, that of comparing average energies and energy fluxes within the loss cone (at the equator) with auroral spectral intensities, could not be accomplished.

Examples of the ATS-6 spectrograms for the "quiet" and "medium-activity" days (shown in Figs. 1 and 2) are shown in Figs. 3 and 4.

3. DMSP Calibration

A complete and detailed calibration of the DMSP imaging system has been achieved. This is the first time an absolute calibration has been obtained, and this will greatly expand the usefulness of these images in auroral and magnetospheric research. A paper reporting these results has been submitted to J. Geophys. Res. and is attached to this report as Appendix I.

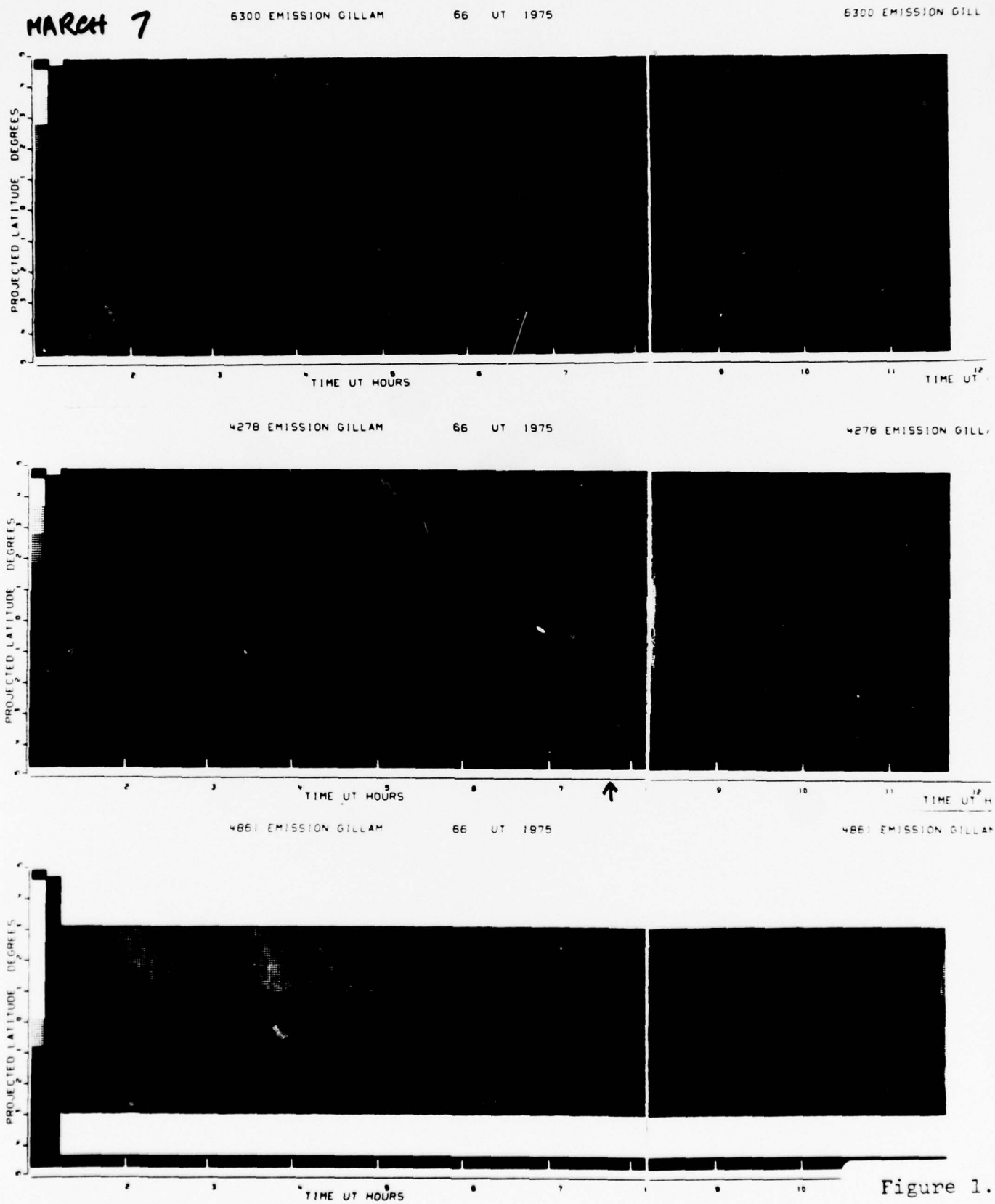
MARCH 7
6300 EMISSION GILLAM 66 UT 1975
6300 EMISSION GILL
PROJECTED LATITUDE DEGREES
TIME UT HOURS
TIME UT
4278 EMISSION GILLAM 66 UT 1975
4278 EMISSION GILL
PROJECTED LATITUDE DEGREES
TIME UT HOURS
TIME UT H
4861 EMISSION GILLAM 66 UT 1975
4861 EMISSION GILLAM
PROJECTED LATITUDE DEGREES
TIME UT HOURS

Figure 1.

3 14

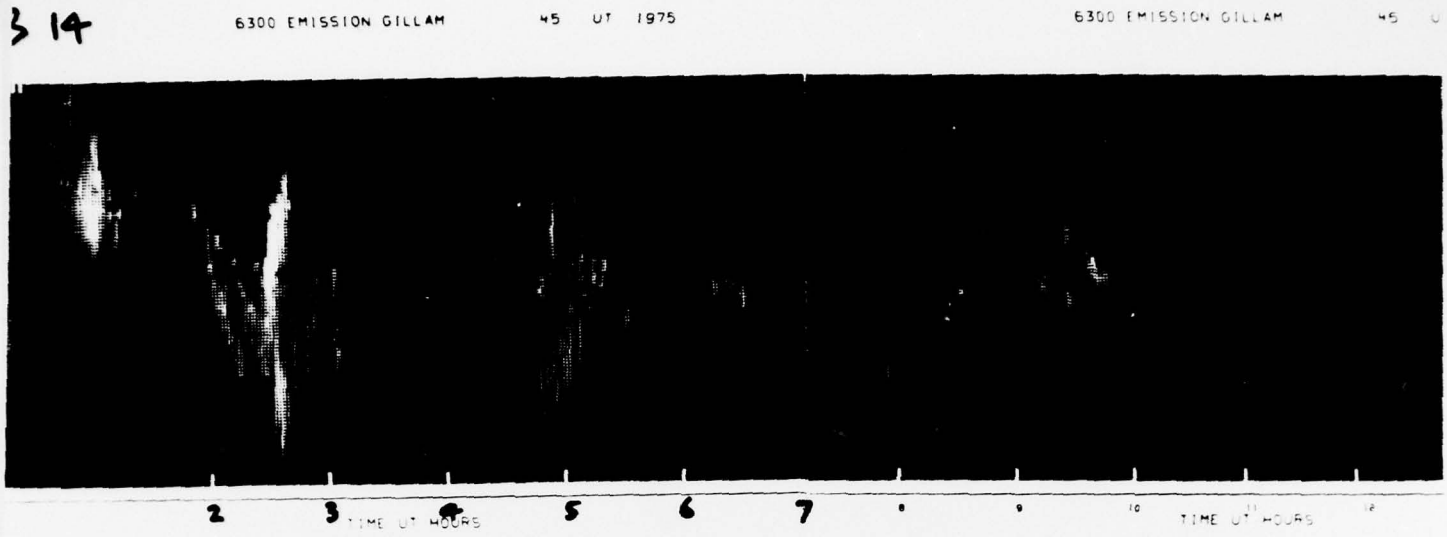
6300 EMISSION GILLAM 45 UT 1975
6300 EMISSION GILLAM 45 U
2
3
5
6
7
TIME UT HOURS
TIME UT HOURS

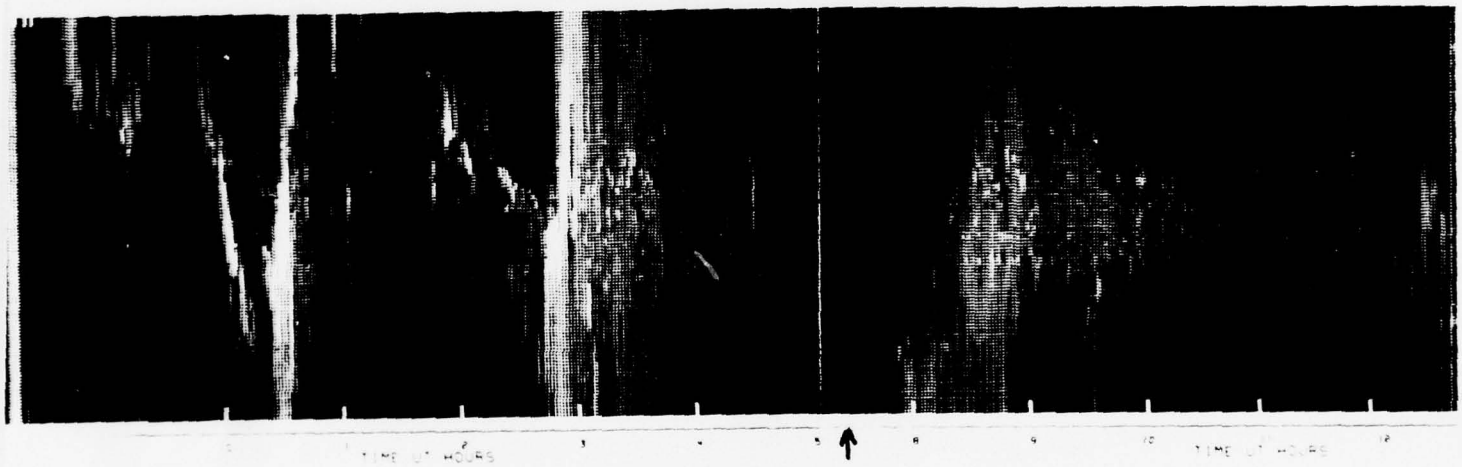
4278 EMISSION GILLAM 45 UT 1975
4278 EMISSION GILLAM 45 U
TIME UT HOURS
TIME UT HOURS

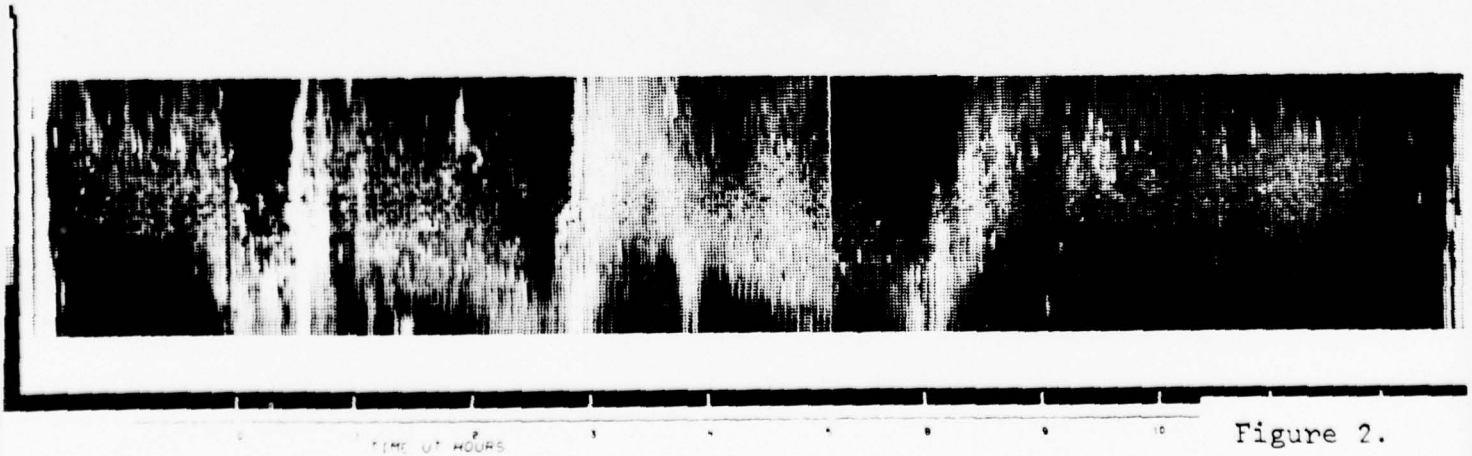
TIME UT HOURS

Figure 2.

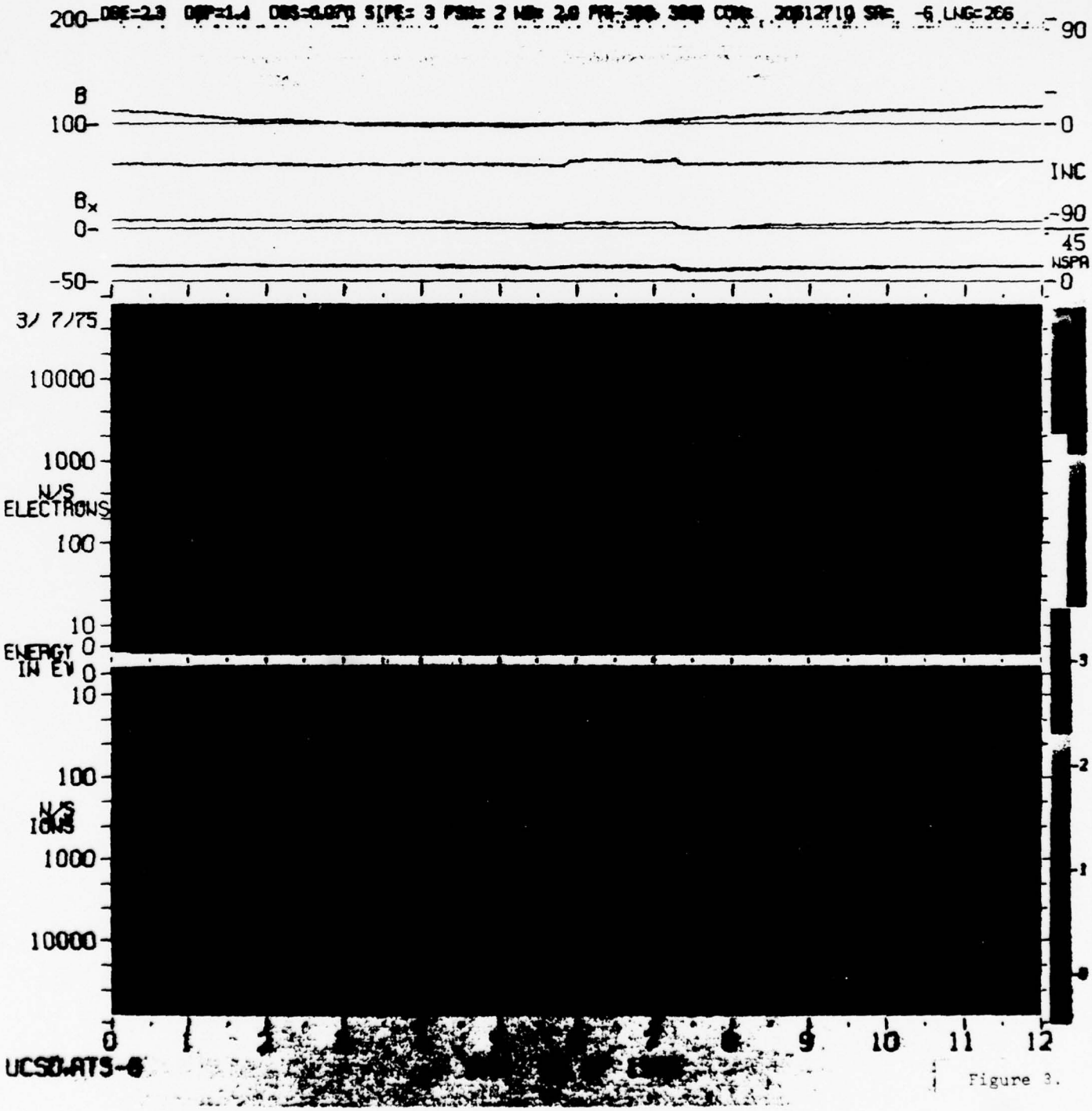
200
90
B
100
0
INC
B_x
0
-90
45
-50
NSPA
0
3/ 7/75
10000
1000
N/S
ELECTRONS
100
10
0
ENERGY
IN EV
0
10
100
N/S
IONS
1000
10000
0
1
2
9
10
11
12
UCSD-ATS-6

Figure 3.

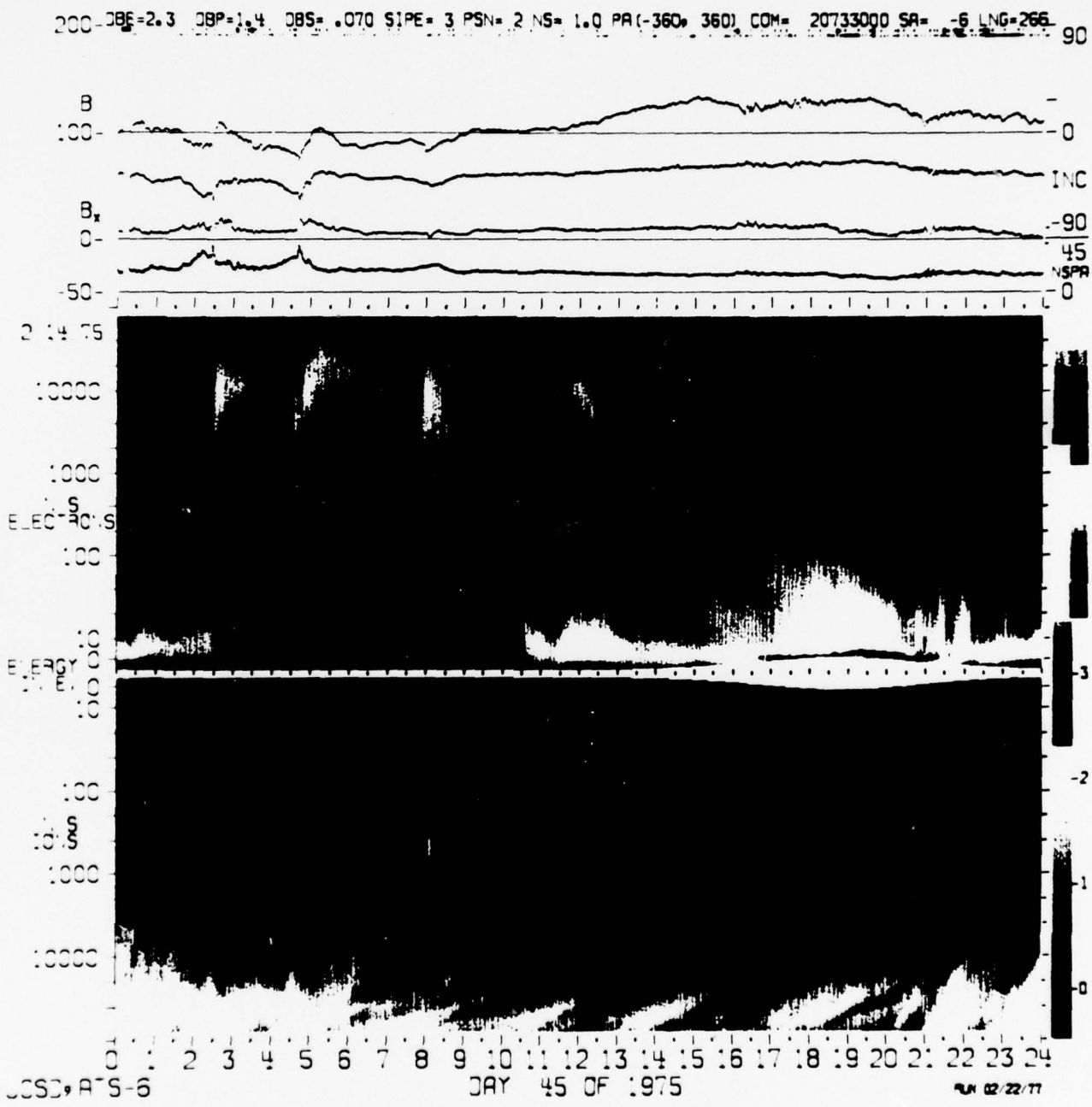
DBE=2.3 DBP=1.4 DBS= .070 SIPE= 3 PSN= 2 NS= 1.0 PA(-360, 360) COM= 20733000 SA= -6 LNG=266
B
INC
NSPA
90
0
-90
45
-50
-3
-2
-1
0 1 2 3 4 5 6 7 8 9 10 11 12 13 14 15 16 17 18 19 20 21 22 23 24
DAY 45 OF 1975
RUN 02/22/77

Figure 4.

DMSP Calibration and the Diffuse Aurora

or

What You Always Wanted to Know About DMSP But Were Afraid to Ask

R. H. Eather

Physics Department
Boston College
Chestnut Hill, MA 02167

Abstract

Although DMSP satellite data is widely used, there has been no reliable absolute calibration. Co-ordinated data with ground-based photometers allow a calibration curve of film density versus 4728 N_2^+ intensity to be derived. The DMSP satellites (5C Series) record airglow, and can detect auroral forms of intensities $\geq$ 50 R of 4278 N_2^+. It is estimated that the 5D Series satellites are capable of detecting auroras with $\sim$25R of 4278 N_2^+. Comparison of "diffuse" auroral images with photometric data show that this form of aurora is excited by a range of proton and electron contributions, varying from almost pure proton excitation to dominant electron excitation.

Introduction

Since 1971, satellite imaging of the aurora has been used to monitor auroral activity on a worldwide basis. The Isis 2 spacecraft has provided spectral imaging, while the USAF Air Weather Service DAPP and DMSP satellites have provided wide-band imaging (extending from the visible through the near infrared). The latter images are currently archived and are available from World Data Service as 35 mm microfilm copies. This ready access has resulted in the DMSP photographs becoming an important resource in auroral and magnetospheric research.

A major problem in using the DMSP images has been the lack of any reliable calibration data, and uncertainty as to what the images represent in terms of the traditionally observed auroral emissions in the visible region. Consequently the DMSP pictures have only been used in a qualitative way, which is an unfortunate underutilization of a high-quality system that has the potential for accurate quantitative use. The purpose of this paper is to present a detailed calibration for one of a DMSP satellite (by co-ordinated comparisons with ground-based photometric measurements), and illustrate the usefulness of the images for quantitative investigations.

The DMSP System

The DMSP satellite system has been described elsewhere (Pike, 1975) so only relevant operational information is summarized here. The system consists of two satellites in sun-synchronous polar orbit (altitude 830 km, inclination 98.75°, period 101.5 mins.), one near the dawn-dusk meridian and the other near the noon-midnight meridian. Images are produced by a line-scanning radiometer which builds up pictures by repetitive scanning across the earth along the orbital

track. Resolution is 3.7 km (center of picture) - 22 km (edge of picture) for the earlier Block 5B/5C satellites and 2.7 km (center) - 5 km (edge) for the Block 5D satellites (operational after March 1977, see Table 1). "Resolution" referred to here is not simply determined by adjacent scanline spacing (as pixel field of view overlaps slightly at nadir, and more at the edge of scan). The better 5D edge resolution is accomplished by a step-function decrease of field of view and variation of the angular sampling rate to compensate for increased ground area in the field of view with increasing slant range.

The following discussion refers to the Block 5B/5C satellites. A number of system changes were incorporated in the later Block 5D satellites, and these are discussed in a later section.

The "visual channel" used for auroral images was sensitive over a band from 4,000 - 11,000 Å for the 5B/5C satellites, with peak response at a wavelength of ~8000 Å (see Figure 1). Each detector had three possible gain states (selection depending on overall light level), and for auroral images the highest gain was used (except in strong moonlight when the medium gain state may have been used). The earlier satellites (Block 5B) only had linear amplifiers, whereas some later satellites (Block 5C) have both linear and logarithmic amplifiers (see Figure 2). Fiducial markings on the photographs show the gain state of the amplifier, but do <u>not</u> indicate whether the amplifier used is in linear or logarithmic mode. This information is apparently no longer available (even from the Air Weather Service), but apart from some initial testing procedures, it appears all the Block 5C satellites

were/are in the logarithmic mode (and highest gain state) for nighttime auroral imaging. Caution should be exercised, however, as there have been periods in recent years when the detector was in the linear mode (because of system testing and because of operational errors).

For Block 5B/5C satellite, d.c. voltage levels from the detector were telemetered to the ground, where they were digitalized into 64 levels, and stored on magnetic tape. (For the Block 5D satellites, 128 digital levels are telemetered directly from the satellite, but the least significant bit is dropped before plotting.) These 64 levels define the gray scale levels for the resulting transparencies. The digital data on tape is only kept for a few days to a week before tapes are recycled.

The gray-scale picture plots are made on any of a number of plotters (three are currently used). Beginning April, 1975 (just after the data reported here were obtained), step-wedge calibration plots were provided daily for each plotter used on that day. The plotter used for each DMSP picture is indicated by the number of small triangles that appear (after June, 1976) between timing information along the edge of the image. To give an indication of the variability between plotters, gray-scale calibrations for three plotters used on April 18/19, 1978 were used to obtain microdensitometer plots shown in Figure 3. Also shown is the nominal gray scale calibration; plotters are supposed to be adjusted to this curve, with an allowed tolerance of ±0.05D. However, it has been found that a density curve which progresses towards white faster than the nominal linear curve produces a much "prettier" picture (clouds

appear whiter rather than gray) so the plotters are often aligned to produce this characteristic. Figure 3 indicates the CDM4 plotter on this day was adjusted to the nominal linear curve, whereas the CDM2 and CDM3 plotters were adjusted for "viewer preference".

It was also found that the gray scale calibration curves vary somewhat across the image. This variation results from the state of adjustment of plotter brightness control in the rectification (linearization of geocentric angle along image scanline) alogrithim, from focus variations, changing optics path, and non-uniform processing. Consequently, for the most accurate work, calibration curves should probably be derived from the same relative location as the data region of interest.

When the original 8" positives are made, they are copied onto 35 mm positive film for the World Data Center, and the originals then retained by Air Force Geophysics Labs. Up until June, 1978, WDC treated this 35 mm copy as their master, from which they made a positive copy. This positive copy was then used to make copies when requested by users. Thus users obtaining 35 mm microfilm from WDC received 4th generation film, with consequent increase in contrast and loss of resolution. At times weak auroras clearly visible on original 8" positives were completely lost (see for example Figure 4a). To improve quality, as of June, 1978, WDC makes user copies from their 35 mm master, so the user now receives 3rd generation film.

The degree of contrast enhancement because of multiple copying is difficult to quantify, as various film types and processing laboratories have been used over the years. Figure 4a illustrates the problem is

serious at times. However, a comparison done in this study of micro-densitometer scans of an original 8" positive and a 4th generation 35 mm positive obtained from WDC (Figure 4b) shows surprisingly good reproduction. The 35 mm copy is clearly of little use for quantitative work, but most auroral features have been preserved.

Previous Calibrations

One of the earliest reports of the DMSP pictures (Rogers et. al., 1974) stated that the minimum detectable signal was 8.5×10^{-10} watt cm^{-2} $ster^{-1}$, and that the system saturated at 8.5×10^{-9} watt cm^{-2} $ster^{-1}$. The lower number has no analytical basis and rests on the subjective assumption that the lowest 10% of the scale at high gain would be "very noisy" and so of "little value". These spectral integrated fluxes are for a solar spectrum (0.4 - 1.1μ) and correspond to about 43 kR and 430kR respectively (along the line of sight of the instrument). These numbers refer to the #5528 Block 5B satellite, which only had linear amplifiers, and so covered only one order of magnitude dynamic range (Figure 2). Although "typical" for the 5B/5C satellites, there was some variation between the various satellites.

Berkey and Kamide (1976) used predicted intensities of auroral emissions (from Vallance Jones, 1971) within the pass-band of the DMSP detector to determine that the threshold sensitivity corresponded to 2-3 kR of the 5577 OI emission and saturation corresponded to 30 kR. A number of nearly coincident passes of the DMSP and Isis 2 satellites allowed them to attempt intercalibration, from which they concluded the DMSP radiometer threshold corresponded to 1.7 - 3.3 kR of 3914 N_2^+ emission. They warned that there is considerable emission below this

threshold and that investigators using DMSP imagery should be cognizant of that fact.

These numbers suggest that the DMSP detector is not as sensitive as all-sky cameras, which typically give useable images corresponding to ~.75 kR of 5577 OI. In the mid-1970's, it became apparent that DMSP images were, if anything, somewhat more sensitive than all-sky cameras. Such conclusions came from qualitative comparison of photographs, and were transmitted by word of mouth rather than by formal publication.

This increased sensitivity of DMSP clearly resulted from the new logarithmic amplifiers. Reference to Figure 2 shows that the 8.5×10^{-10} - 8.5×10^{-9} watts cm^{-2} $ster^{-1}$ operational range of the linear detector results in a channel output voltage of 0.6 - 7.2 volts. This same output voltage range corresponds to 1.6×10^{-10} - 8.5×10^{-9} watts cm^{-2} $ster^{-1}$ for the logarithmic amplifier, representing an increase in sensitivity of a factor of 5, an increase in dynamic range to ~50, and the same saturation level. Thus according to Berkey and Kamides (1976) numbers, we would expect a threshold level of ~300-600 R at 3914 N_2^+, and saturation at ~25 kR (uncorrected for albedo).

Mende and Eather (1976) reported an intercalibration of DMSP (#8531 with logarithmic amplifier) with ground based photometers. They concluded that DMSP gave a useable image when auroral intensity reaches 150 R at 4278 N_2^+ (corresponds to 450 R at 3914 N_2^+), but that the picture saturated at ~500 R 4278 N_2^+. It will be shown in this paper that DMSP sensitivity is in fact as low as 50 R at 4278 N_2^+, and saturation occurs at ~2.5 kR. The discrepancy with the previous work results from the present use of original 8" formal DMSP positives, rather than the 4th generation copy prints obtained from World Data Center microfilm for the

earlier study.

Airglow and Continuum

With the wide spectral band detectors used on DMSP, the integrated airglow and continuum emissions is appreciable. The principal airglow emissions are the atomic oxygen lines, the O_2 atmospheric system, and the hydroxyl system. Expected intensities (Roach and Gordon, 1973) are shown in Figure 1b, together with the detector response curve. Integration over the response curve gives about 18 kR. To this should be added that contribution from reflected starlight, zodiacal light and gegenschein, which might be expected to add another 2-3 kR (Roach and Gordon, 1973). Assuming an albedo of ~1.0 for the snow covered arctic, and allowing for atmospheric transmission effects (Nawrocki and Papa, 1963), we estimate that DMSP will see about 30-35 kR. This total "background" emission will trigger the first 30% of the dynamic range of the system (see Figure 2) and so result in an overall background density on the film of ~1.15 D (See Figure 3).

The above comments apply on moonless nights. Background levels will, of course, rise dramatically under lunar illumination and result in considerable loss in ability to detect weak auroral emissions.

At this point it is of interest to calculate the auroral intensity needed to equal this airglow/continuum contribution. Reference to Figure 1a gives that a total auroral intensity of 33 kR (integrated over detector response and with some albedo and transmission assumptions as above) corresponds to a 5577 OI intensity of ~670 R. Reference to Figures 2 and 3 shows that if this is added to the airglow/continuum

the DMSP image density should change by about 0.2D to 0.95D. Weak auroral images will appear as low-contrast enhancements (diffuse borders) on the background density, which is typically quite grainy. A human observer should be able to readily identify a 0.05D change under such conditions, which corresponds to ~170 R 5577 OI. This should represent an estimate of the ultimate sensitivity of the DMSP system i.e., an aurora of ~170 R 5577 OI should be just detectable. (This corresponds to ~100 R 3914 N_2^+ or ~35 R 4278 N_2^+.)

A four-channel meridian-scanning tilting-filter photometer system was operated from Gillam, Manitoba (66.2°N, 323.4°E geomagnetic) in February-March, 1975 for co-ordinated measurements under the ATS-5 and ATS-6 satellites. During this period, there were 20 cases of simultaneous DMSP and photometer data on clear, moonless nights, with Gillam appearing near the central part of the DMSP picture and auroras in the field of view.

The photometer scanned ±80° from the zenith, with a north-south scan taking 90 secs. The time of DMSP passage across the Gillam meridian was determined, and the photometer scans immediately before, during, and after this time were used to compare with microdensitometer plots from the original DMSP 8" positives. The microdensitometer scan was made along the projection of the photometer meridian scan at the 100 km level on the DMSP picutre. (Gridding procedures are explained by Pike, 1975.) Microdensitometer spot size was adjusted to roughly match the 3° field of view of the photometers. (In most cases it was possible to identify the town lights of Gillam on the DMSP picture, and the image of these lights gave a corresponding peak on the micro-

densitometer scan.) Photometric ratios were used to derive heights of emission, and hence latitude, as in our standard keogram program (Eather et. al., 1975). Calculated field-aligned photometric intensity can then be plotted as a function of latitude.

A logarithmic density range of 0.05 → 2.1D was necessary to span the transmission range from the clearest part of the DMSP positive (fog level) to fully saturated black. The saturated black was down the sides of the film (various fiducial marks etc.), and the "blackest" part of the DMSP images corresponded to a density of ~1.2 D; this density level corresponds to the integrated airglow signal.

"Weak" Auroral Arcs: An example of co-ordinated data for very weak auroral conditions is shown in Figure 5. The region of the photometer scan is marked on the DMSP picture, which is a contact print from the original positive. The diffuse aurora in the bottom part of the picture is stable and does not change during the three photometer scans. The structured arc at the top of the picture is clearly moving and transient, as it only shows in the photometer scan before the co-ordination time, and then was at a lower latitude than when detected by DMSP.

The overall background density of the DMSP positive is about 1.2D (and this was true for all positives examined). The diffuse arc image appears above this, and it corresponds well with the photometer data. 4278 N_2^+ intensities exceeding ~40 R are seen to give a DMSP density above the 1.2D background. Peak 4278 N_2^+ intensity of 120 R corresponds to a film density of about .95D.

Also plotted in Figure 5 is the H_β intensity. The ratio of

4278 N_2^+/H is ~1.5, which implies that all of the observed diffuse aurora can be excited by precipitating protons (Eather, 1968). The narrow structured arc on the northern edge of the diffuse aurora is too narrow to be excited by protons (because of charge-exchange spreading), so that arc, together with the transient arc to the north, must be primarily electron excited.

Three more examples of weak arcs are given in Figure 6a, b, c. In Figure 6a, the double structure of the diffuse arc is not resolved by the photometer keogram program (which is understandable if one considers the vertical distribution of emissions and geometry of the arcs with respect to the station). The H_β plot and 4278 N_2^+/H_β ratio of ~4. show, that both electrons and protons contribute to diffuse aurora excitation, though the region of hydrogen emission is broader. In Figure 6b, the northernmost intense structure is clearly transient; the patchy aurora over Gillam is also undergoing short term changes; the diffuse aurora to the south is stable, and the ratio of 4278 N_2^+/H_β (~4) indicates protons and electrons contribute about equally to its excitation, with the hydrogen emissions broader in latitude. In Figure 6c, the strong northern arc is transient and must have only existed by <90 seconds, just as the satellite was passing over that location. The stable diffuse aurora seems to be largely excited by electrons on its northern half and protons on the southern half.

"Medium" Auroral Arcs: Figure 7a, b, c gives examples of more intense auroral forms. In Figure 7a, there is an overall background level of ~180 R of 4278 N_2^+ which gives a film density of ~0.83D.

About 1/3 of this seems to be proton excited, and the remainder must be widespread low intensity electron precipitation. Superimposed on this to the south of Gillam is a double-structured diffuse form excited by a combination of electrons and protons, and temporal changes are evident in the electron component. In the example of Figure 7b, most of the ~300 R 4278 N_2^+ across the picture can be attributed to the broad diffuse proton precipitation, giving H_β ~100 R. The electron-excited structures that superimpose vary in time, so detailed correlations are difficult to make, though the arc almost overhead at Gillam is identifiable in the DMSP and photometer trace corresponding to the satellite being overhead. 4278 N_2^+ intensity of ~1000R gives a film density of ~.37D. Figure 7c shows a localized temporal structure in the north (not seen by the photometer), a changing but well correlated structure in the center of the picture, and a stable diffuse aurora to the south which seems dominantly proton excited but with some superimposed electron structure.

"Strong" Auroral Arcs: Figure 8a, b, c shows examples of auroras that are intense enough to saturate the DMSP film. In Figure 10a, the DMSP is just on the verge of saturation, and this is seen to correspond to a 4278 N_2^+ intensity of 2.75 kR. The strong diffuse aurora in the south (~130 R H_β, 800 R 4278 N_2^+) is excited by both protons and electrons. Figures 8b and 8 c show similar examples, with some DMSP peaks being transient auroras that are missed by the photometer.

Calibration Curve

The 20 cases of co-ordination (of which 10 have been presented here) were examined and all cases of definite correlated structures used to plot

the calibration curve of Figure 9. As previously mentioned, no gray-scale calibration data was available at this time. Fortunately all DMSP pictures in this study were generated on the same plotter, so there is not the uncertainty of different calibrations for different plotters (Figure 3). However, part of the scatter in Figure 9 could result from a changing calibration of the plotter with time, as these data cover a six week period. The continuous-drive wet process used does not receive good quality control and maintenance, and chemical residues in the system are common, sometimes leading to solid matter on the dried films.

It may be seen that a consistent calibration relationship is apparent. We conclude that absolute intensities may be derived from the original DMSP positives, within an accuracy of ~±50%. Minimum detectable intensity f[illegible]tellite was ~50 R of 4278 N_2^+, with saturation of ~2.5 kR. The DMS[illegible]ata has not been corrected for albedo, which is expected to be ~1.0 for the uniform snow covered surface of northern Manitoba. This effectively increases the absolute sensitivity of DMSP, but as albedo affects the background airglow signal also, it does not change the signal/noise ratio that determines the minimum detectable auroral intensity. We argued above (in the section of Previous Calibrations) that the expected threshold for the logarithmic detectors should be 300-600 R at 3914 N_2^+, which corresponds to 100-200 R at 4278 N_2^+. Given the effect of albedo, this corresponds to 50-100 R as measured for the same aurora from the ground. The agreement of this estimate with the experimentally determined 50 R is better than anyone had any right to expect.

Note too that there is a van Rhijn effect (the increase in optical thickness because of increased obliquity of the view angle) in the DMSP photographs. Depending on the height distribution of the aurora and the geometry of the situation, this can give a factor of ~2 enhancement near the east and west edges of the picture. This was not allowed for in this analysis as in most cases Gillam was nearer the center of the picture. (The effect is, however, allowed for in the program that analyzes the photometer data - this is necessary because of high obliquity in ground based measurements for aurora still near the central part of the DMSP pictures.)

Warning Concerning Temporal Fluctuations

We have mentioned a number of cases above where auroral forms on the DMSP pictures are not recorded on the photometer scans, implying that they existed for <90 seconds (the meridian scan time of the photometer), so appeared briefly at their recorded position when DMSP was overhead at that location. In most cases both temporal and spatial effects are probably important.

Usually examination of the shape of the form indicates it was probably a transient brightening (see for example the northern forms in Figures 4b, 5, 6) but sometimes what looks like a stable arc form on the photograph was in fact a transient phenomena. Such was the case published by Mende and Eather (1976) and repeated here as Figure 10. The well defined arc just south of the zenith at Gillam in the picture actually formed north of Gillam, quickly moved south, then faded, all within a 3 minute time interval. There were no other discrete auroras

recorded by the photometer within ±20 minutes of this event. This example is presented simply to illustrate the possible pitfalls in assuming longevity and stability of discrete auroras recorded by DMSP.

Subsequent Satellites

The calibration curve presented here is for the 5C/8531 satellite. The other 5C satellites (#9531 and #10533) also used radiometer detectors, and should have very similar calibration curves. The 5D satellites have photomultiplier detectors with less red response than the radiometer (silicon diode) detectors. Although the quantum efficiency of photomultipliers (peak ~25%) is much lower than for silicon diodes, the signal/noise characteristics at low light levels are far superior.

Normalized response curves for some 5D detector channels (including optics), are shown in Figure 11a. F1 to F3 used modified extended S-20 photocathodes, whereas the F4 and F5 instruments use cesiated gallium-arsenide photocathodes for extended red response, and a yellow filter to limit blue response. Peak quantum efficiencies are ~22% for trialkali tubes, and ~15% for GaAs tubes.

The calibration curve for the F3 detector shown in Figure 11b illustrates the characteristics of the 5D system. The photomultiplier detector is switched in line when radiance falls below about 5×10^{-5} watts cm^{-2} $ster^{-1}$, and then switched to a higher gain state at about 4×10^{-7} watts cm^{-2} $ster^{-1}$. (Radiance is a spectral integration over the solar spectrum between 0.4 and 1.1μ.) Plotted in Figure 11b is the Variable Digital Gain Amplifier (VDGA) gain, which has a 64db dynamic

range (dB = 20 x log (ratio)). For a given VDGA gain, the plot gives the radiance that results in saturation of the amplifier.

Normally for auroral images, the PMT detector is in a logarithmic mode, with a dynamic range of 40db. Thus at face value Figure 11b shows that when the VDGA amplifier gain is near its maximum of 64db, the detectable input would be 40db down on $\sim 5 \times 10^{-9}$ watts cm^{-2} $ster^{-1}$ i.e. $\sim 5 \times 10^{-11}$ watts cm^{-2} $ster^{-1}$. However, detector noise has been measured in orbit with a known intensity LED source, which gives a S/N ratio of 1.0 for a radiance of $\sim 5 \times 10^{-10}$ watts/cm^2 ster. Expected airglow levels are about 1.5 times this radiance, and so effectively set the low limit for auroral detectability.

To estimate the relative sensitivity of the 5D and 5C series instruments to an auroral spectrum, we folded the detector spectral responses into the predicted auroral and airglow/continuum spectra shown in Figs. 1a, 1b, and Table 1 shows the results.

Table 1

Satellite Number	Spectral Integrated Flux (kR)		% Contribution of 5577 OI
	IBC 2 Aurora	Airglow	
5C/8531 5C/9532 5C/1053	150	20	3.3
5D/12535 (F1)	64	4.5	15
5D/13536 (F2)			13
5D/14537 (F3)			12
5D/15538 5D/16539 (not yet launched)	73	7.2	11

Table 1 shows that the reduction in auroral response of the 5D detector (because of its decreased spectral range) is a factor of 2 - 2.5. However,

the relative contribution of aurora to airglow is better for the 5D detector. If we define the "ultimate auroral sensitivity" of the detector as its ability to detect low auroral intensities above airglow, we estimate the current 5D PMT detectors should be perhaps twice as good as the 5C detector, and so should be capable of detecting aurora characterized by ~25R of 4278 N_2^+. Future 5D detectors with increased red response should be capable of detecting aurora characterized by ~35-40R 4278 N_2^+.

Unfortunately some other features of the 5D instruments make it less desirable as an auroral imager. There are three modes of gain control:

(i) Along scan: gain is adjusted for each pixel from a program that calculates solar elevation wrt viewing region. At quarter moon and above, expected lunar illumination as a function of solar elevation is calculated, and used to control gain.

(ii) Along track: gain is optimized for solar/lunar elevation each scan at subsatellite point.

(iii) Preset: gain is constant for picture.

Modes (i) and (ii) are to optimize cloud pictures and will normally be operative for solar elevations above -28°, though may also be in use for some auroral images (especially if there is lunar illumination). Such automatic gain changes (in increments of 1/8 db) would make it virtually impossible to derive quantitative auroral intensities. But normally for new moon conditions, the detector should be in mode (iii) for auroral images, and there are 64 possible preset gains, adjustable from 0 to 63db in 1db steps. The gain mode and gain state of the detector is coded down the side of the DMSP positives, with ½db resolution (see Figure 12).

Another problem arises from switching of the pixel field of view on the 5D satellites. Because of increasing distance to the earth at the edges of the pictures, the resolution at constant field of view would be

down by a factor of 6 at the picture edge (as were the 5C pictures). The 5D instrument changes to a smaller field of view about 1/3 of the way out from the center of the picture, and reduces the variation in pixel resolution to a factor of 2. When field of view is decreased, less light enters the detector so amplification is simultaneously adjusted to compensate. This compensation has never been particularly successful and as a result, the center part of auroral pictures is effectively at a different gain than the edges. This step change is very obvious (see Figure 13) and would have to be allowed for in quantitative work.

Conclusions

Tracking down the chain of events and calibration variables between the DMSP detector and the film supplied to users has been interesting detective work. There is no central documentation source and much of the information has been uncovered by word of mouth. Perhaps this situation is not surprising; the DMSP system is a real-time operating Air Force system which, besides supplying meteorological cloud data, is used to provide auroral positional data to an ionospheric prediction program for real-time communications applications. The system was not designed for quantitative auroral reasearch, and the Air Force has been most co-operative in making auroral data available to the scientific community.

The so-called "diffuse aurora" was originally identified and categorized from ISIS pictures (Lui et. al., 1973). From the characteristics and location of this diffuse belt, it seemed that it was the region of proton aurora, and insistence on a new term to describe this region (simply from its appearance on the DMSP photographs) has led to considerable confusion. Nagata et. al. (1975) demonstrated that the diffuse auroral belt always coincided with the H_β emission belt, and that the correspondence was "perfect and without exception." The present study confirms that conclusion, but the quantitative data shows that protons are not always the dominant energy source in this region. We believe this "diffuse aurora" is a combination of steady plasma-sheet drizzle of protons and electrons, modified after injection events by particle loss from the reconstituted plasma sheet of freshly injected, azimuthally drifting protons and electrons (Eather et. al., 1975). Proton drift

paths after injections can lead to regions of essentially pure proton precipitation. Consequently the proton/electron ratio of precipitating particles in proton auroras (or diffuse auroras) is variable and depends on the recent time history of substorm injections.

The DMSP detector is a high quality instrument, and can be used profitably in a quantitative fashion if users are aware of possible pitfalls. If users know in advance of requirements for data at special times, a request might be made to assure a desired gain mode and gain setting, and to preserve the digital tapes for superior quantitative data. Computer processing of such data, or of digitized data regenerated from DMSP positives, could be used to determine total energy inputs, or to derive intensity contour maps for quantitative comparison with other measurements. Thus, reliable absolute calibrations can greatly expand the usefulness of these photographs in auroral and magnetospheric research.

Acknowledgements

I would like to thank Al Kimball at Westinghouse and Lt. Col. L. Snyder at Air Force Geophysics Labs., for explanations of many features of the DMSP system. This research was supported by the Air Force Office of Scientific Research under Contract F44620-76-C-~~0219~~0129.

References

Berkey, F.T. and Y. Kamide, On the distribution of global auroras during intervals of magnetospheric quiet, J. Geophys. Res. 81, 4701, 1976.

Eather, R.H., Spectral intensity ratios in proton-induced auroras, J. Geophys. Res. 73, 119, 1968.

Eather, R.H., S. B. Mende and R.J.R. Judge, Plasma injection at synchronous orbit and spatial and temporal auroral morphology, J. Geophys. Res. 81, 2805, 1976.

Lui, A.T.Y., P. Perraut, S.-I. Akasofu, and C.D. Anger, The diffuse aurora, Planet. Space Sci., 21, 857, 1973.

Mende, S.B. and R.H. Eather, Monochromatic all-sky observations and auroral precipitation patterns, J. Geophys. Res. 81, 3771, 1976.

Nagata, T., T. Hirasawa and M. Ayukawa, Discrete and diffuse auroral belts in Antarctica, Rept. Ionos. Res. Japan, 29, 149, 1975.

Nawrocki, P.J. and R. Papa, "Atmospheric Processes," p. 10.10, (Prentice Hall, N.J.), 1963.

Pike, C.P. (editor), Defense meteorological satellite program auroral-ionospheric interpretation guide, Air Force Surveys in Geophysics No. 306, AFCRL, April 4, 1975.

Roach, F.E. and J.L. Gordon, "The Light of the Night Sky," (D. Reidel, Dordrecht, Holland), 1973.

Rogers, E.H., D.F. Nelson and R.C. Savage, Auroral photography from a satellite, Science 183, 951, 1974.

Vallance Jones, A., "Aurora," (D. Reidel, Dordrecht, Holland), 1974.

Figure Captions

Fig. 1a. Intensities of the main auroral emissions, for IBC2 Aurora (5577 OI = 10 kR), from Vallance Jones (1974). Also shown is the spectral response of the DMSP radiometer used on Block 5B/5C satellites. The histogram shows the fraction of the total auroral response in 1000 Å wavelength intervals. The dashed curve is a typical response characteristic (normalized) for all-sky camera (panchromatic) film.

Fig. 1b. Intensities of the main airglow emissions, from Roach and Gordon (1973). Also shown is the spectral response of the DMSP radiometer used on Block 5B/5C satellites.

Fig. 2. Representative response curves of the linear and logarithmic amplifiers on the Block 5B/5C DMSP satellites. The radiance is spectrally integrated over a solar spectrum.

Fig. 3. Film density versus step wedge number for the calibration film supplied with DMSP film on April 18/19, 1978. The CDM number defines the plotter used to generate the calibration gray scale.

Fig. 4a. Contact print from original DMSP 8" positive, shows weak aurora over Greenland on December 28, 1976. On the right is an enlargement of the copy frame provided on 35 mm microfilm from World Data Center.

Fig. 4b. Comparison of microdensitometer plots from original DMSP 8" positive, and from 35 mm microfilm obtained from World Data Center, for

February 13, 1975. Also shown is a contact print from the original, and an enlargement from the microfilm.

Fig. 5. Contact print from original DMSP 8" positive, microdensitometer plot, and corresponding ground based photometer data, for Orbit 4751 of satellite 8531, February 14, 1975. The meridian-scanning photometer scans along the direction marked on the DMSP photograph, which is the track scanned by the microdensitometer. The dashed peak on the micro-densitometer plot is the town lights of Gillam and a nearby dam construction site, seen as two dots in the center of the meridian scan marked on the DMSP picture. Three photometer scans at 4278 N_2^+ are shown: --- is the scan just before DMSP was overhead, —— is the scan during which DMSP passed overhead, xxx is the scan just after DMSP was overhead. The H_β region is shaded.

Fig. 6a, b,c Further examples of coordinated data for "weak" auroral forms. See legend for Figure 5.

Fig. 7a, b,c Examples of coordinated data for "medium" intensity auroral forms. See legend for Figure 5.

Fig. 8a, b,c Examples of coordinated data for "strong" auroral forms. See legend for Figure 5.

Fig. 9. Calibration curve derived from coordinated data where auroral forms are clearly correlated on the DMSP and photometer data.

Fig. 10. DMSP picture for February 13, 1975. Also shown are representative photometer scans before, during, and after the satellite overpass,

to illustrate the temporal nature and spatial movement of the seemingly steady arc seen in the picture.

Fig. 11a. Spectral response of some of the PMT detectors used for the Block 5D satellites.

Fig. 11b. Amplifier gain required to give 100% output (saturation) for the indicated radiances, for the F3 detector. The radiance is spectrally integrated over a solar spectrum.

Fig. 12. Explanation of coding of time, gain mode, gain level, and gain trend on Block 5D images. This coding strip appears along the right-hand edge of the images.

Fig. 13. Examples of discontinuities introduced by switching of pixel field of view.

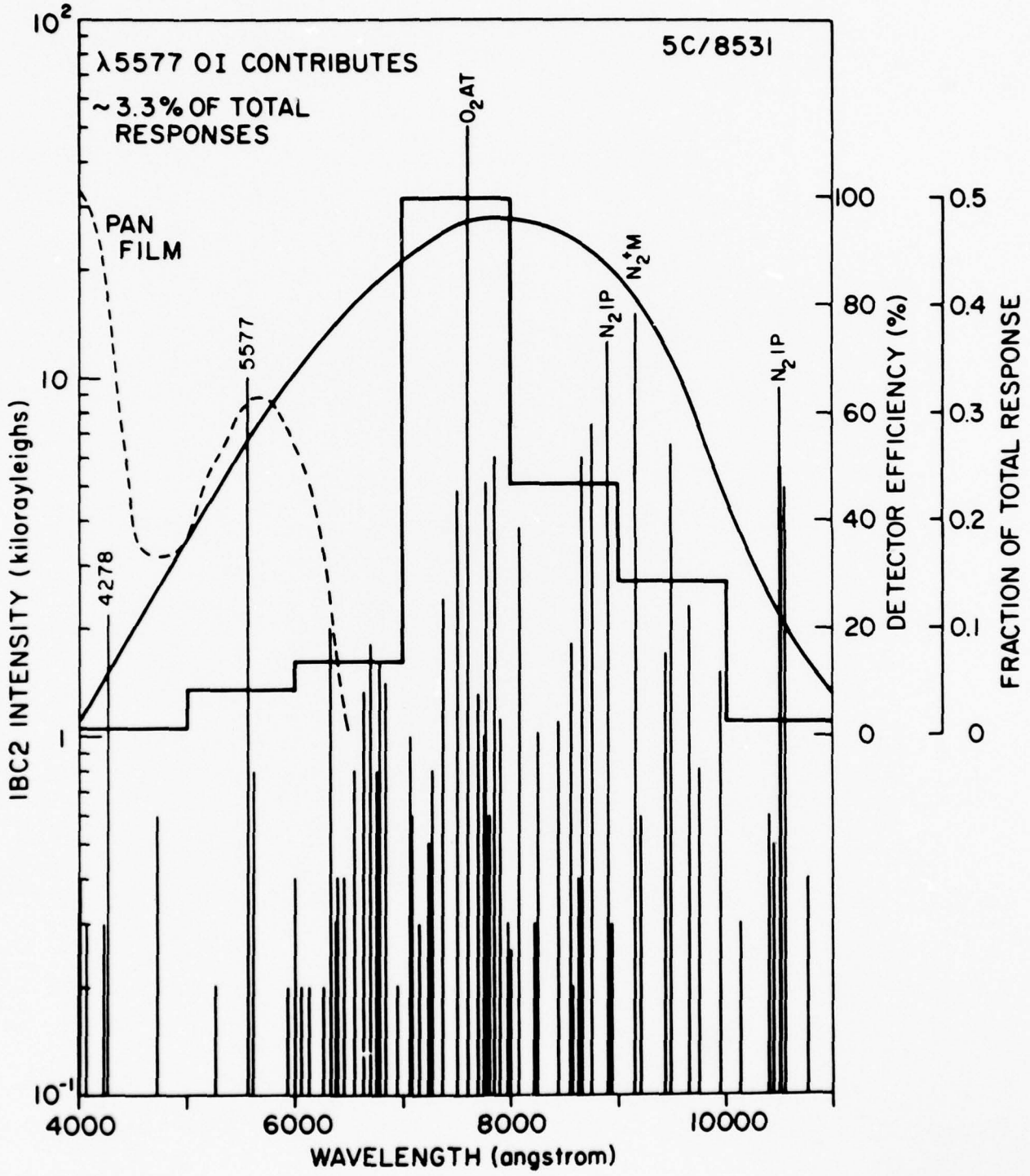
5C/8531
λ5577 OI CONTRIBUTES
~3.3% OF TOTAL
RESPONSES
PAN
FILM
O_2 AT
N_2^+M
N_2 1P
N_2 1P
5577
4278
10^2
10
1
10^{-1}
IBC2 INTENSITY (kilorayleighs)
100
80
60
40
20
0
DETECTOR EFFICIENCY (%)
0.5
0.4
0.3
0.2
0.1
0
FRACTION OF TOTAL RESPONSE
4000
6000
8000
10000
WAVELENGTH (angstrom)

Figure 1a.

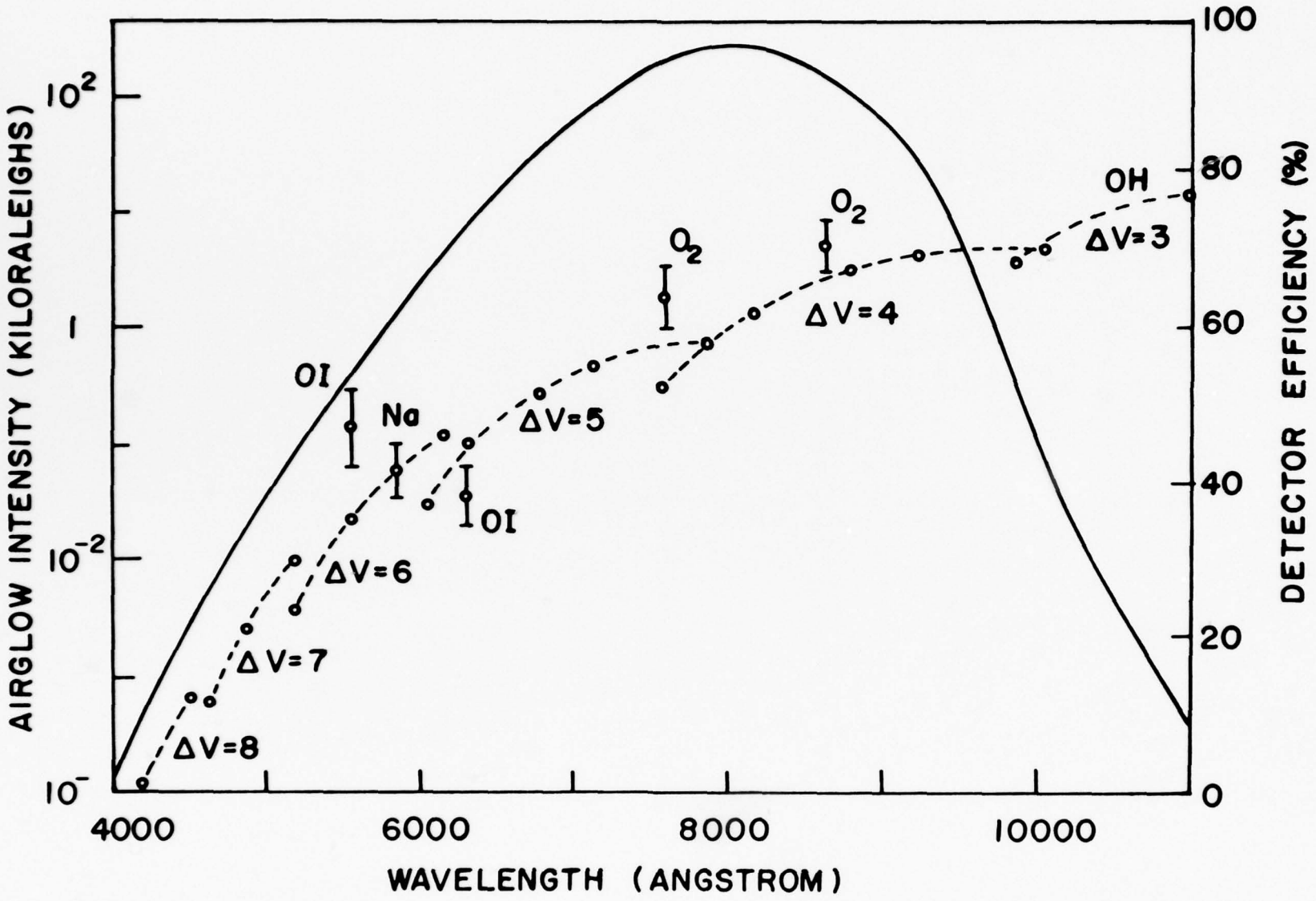
AIRGLOW INTENSITY (KILORALEIGHS)
10^2
1
10^{-2}
10^{-}
DETECTOR EFFICIENCY (%)
100
80
60
40
20
0
4000
6000
8000
10000
WAVELENGTH (ANGSTROM)
OI
Na
OI
O_2
O_2
OH
ΔV=8
ΔV=7
ΔV=6
ΔV=5
ΔV=4
ΔV=3

Figure 1b.

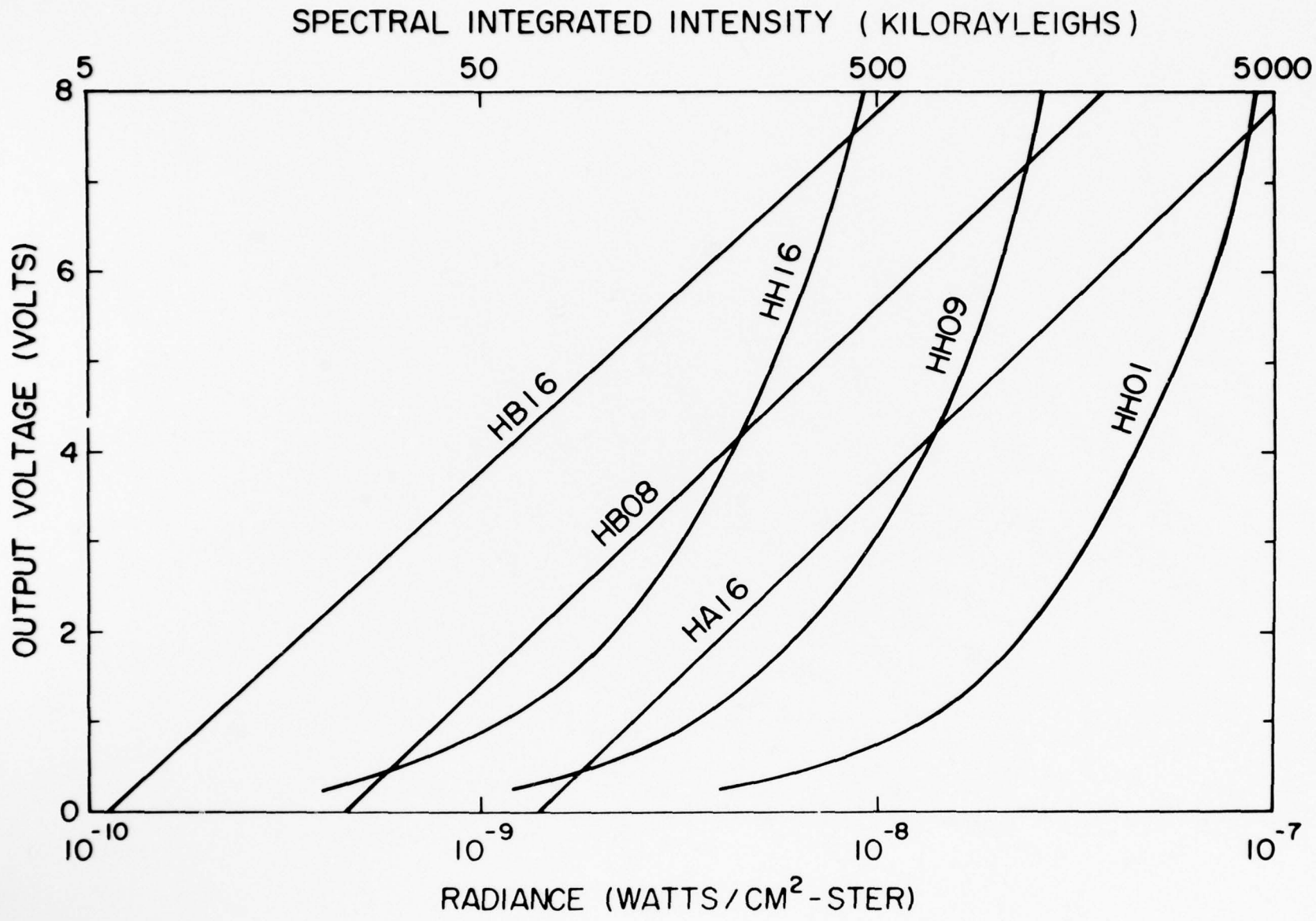
SPECTRAL INTEGRATED INTENSITY (KILORAYLEIGHS)
5
50
500
5000
OUTPUT VOLTAGE (VOLTS)
8
6
4
2
0
HB16
HH16
HB08
HH09
HA16
HH01
10^{-10}
10^{-9}
10^{-8}
10^{-7}
RADIANCE (WATTS / CM^2 - STER)

Figure 2.

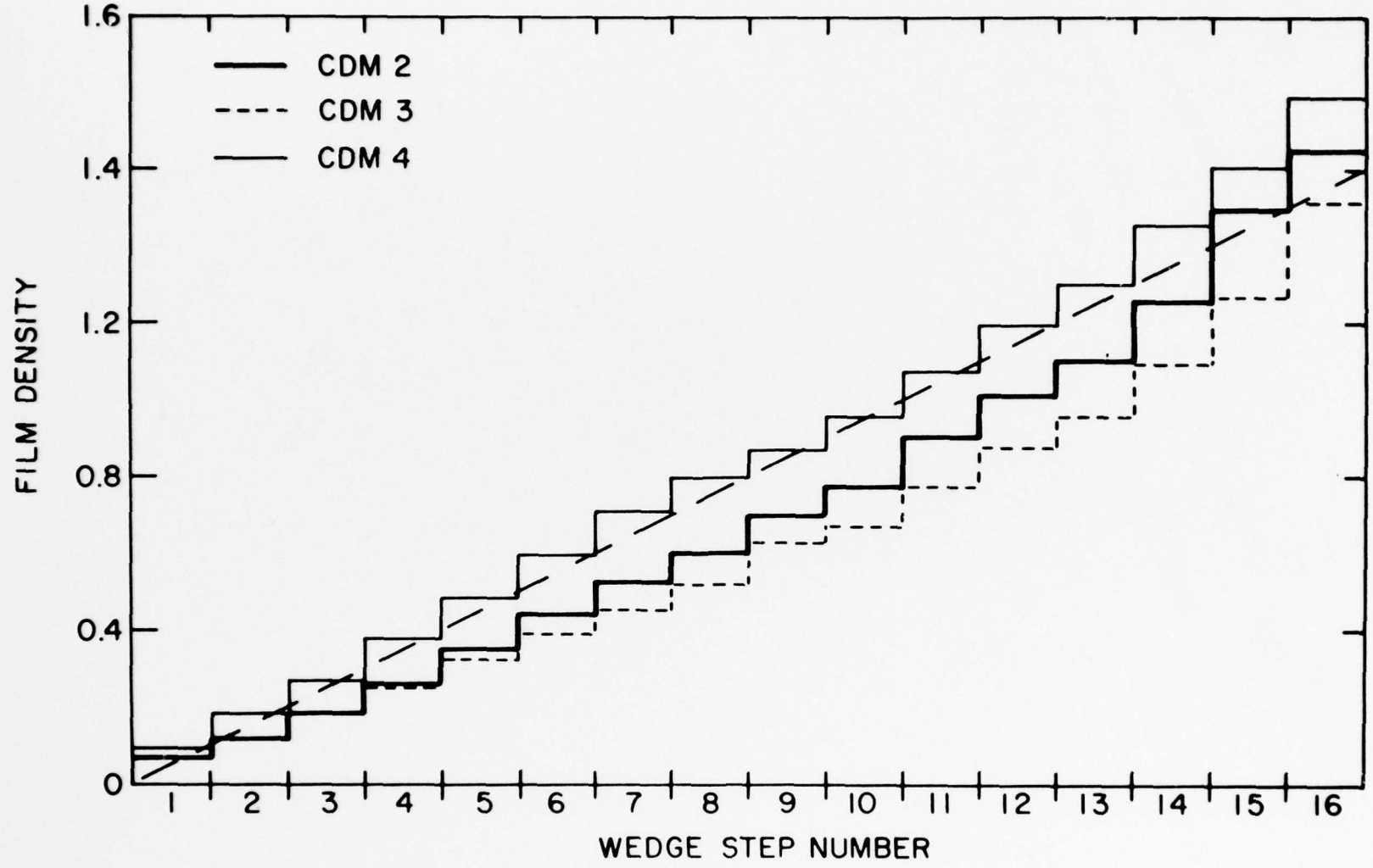
CDM 2
CDM 3
CDM 4
FILM DENSITY
1.6
1.4
1.2
0.8
0.4
0
1
2
3
4
5
6
7
8
9
10
11
12
13
14
15
16
WEDGE STEP NUMBER

Figure 3.

Figure 4a.


3/13/75 0734 UT
ORBIT 5134

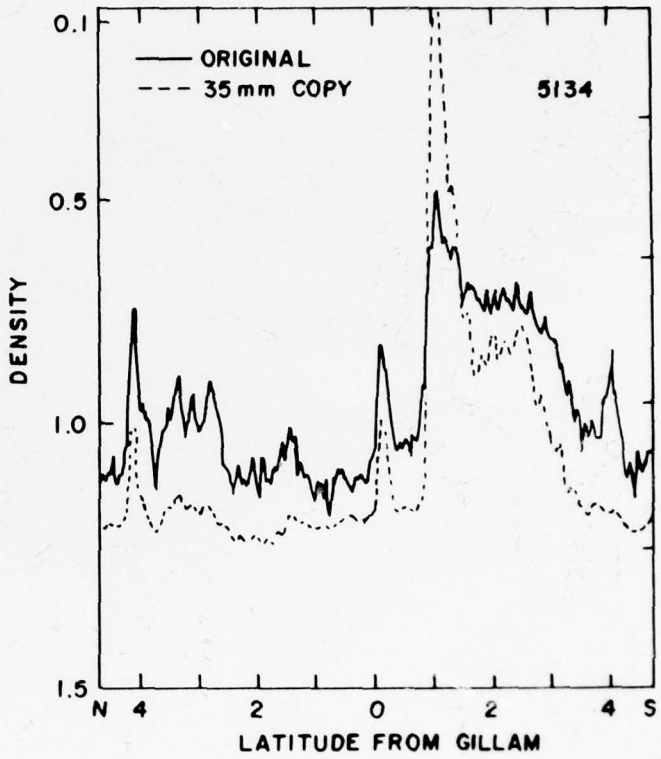
ORIGINAL
35 mm COPY
5134
DENSITY
0.1
0.5
1.0
1.5
N 4 2 0 2 4 S
LATITUDE FROM GILLAM

Figure 4b.

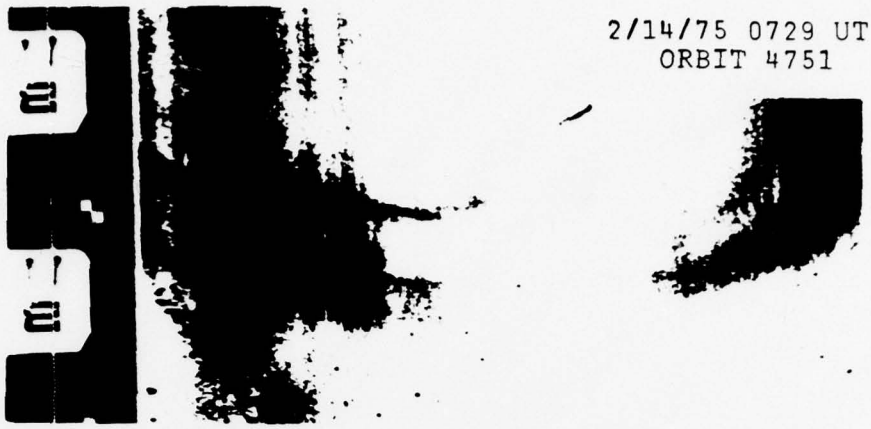
2/14/75 0729 UT
ORBIT 4751

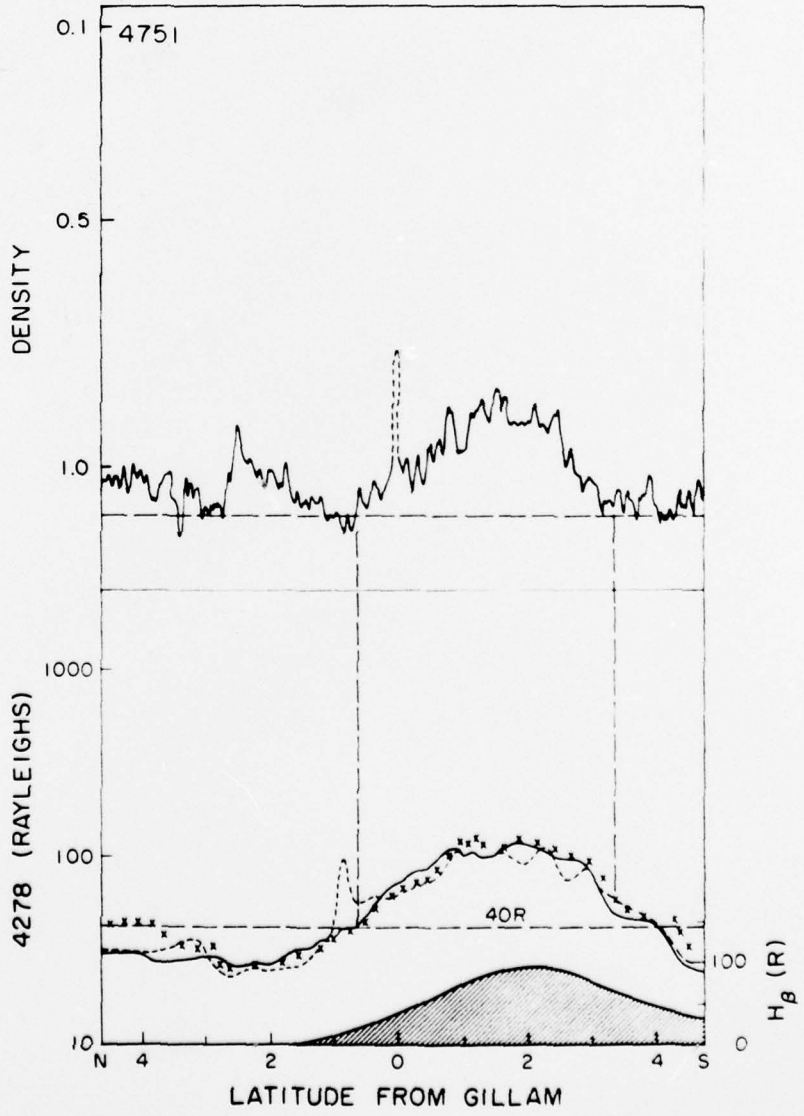
4751
0.1
0.5
1.0
DENSITY
1000
100
10
4278 (RAYLEIGHS)
40R
100
0
H_β (R)
N 4 2 0 2 4 S
LATITUDE FROM GILLAM

Figure 5.

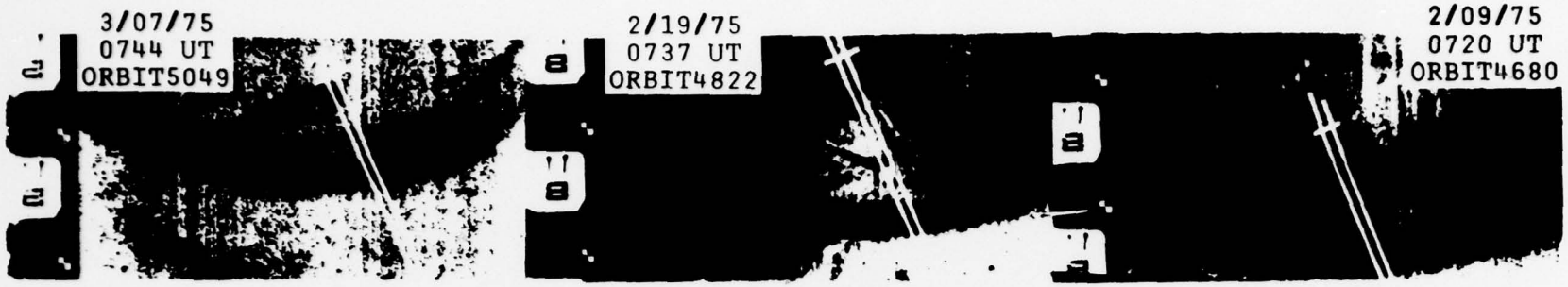
3/07/75
0744 UT
ORBIT5049
2/19/75
0737 UT
ORBIT4822
2/09/75
0720 UT
ORBIT4680

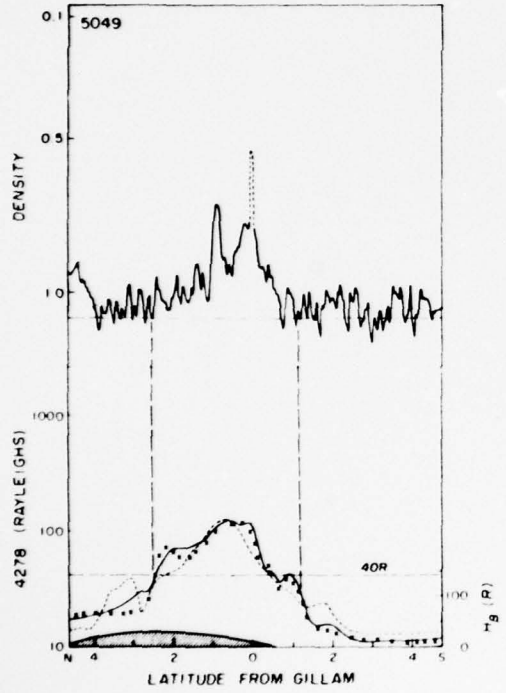
5049
DENSITY
4278 (RAYLEIGHS)
40R
LATITUDE FROM GILLAM

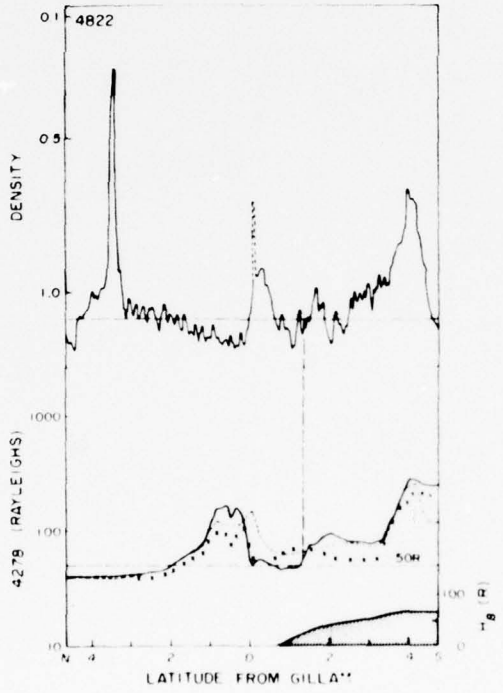
4822
DENSITY
4278 (RAYLEIGHS)
50R
LATITUDE FROM GILLAM

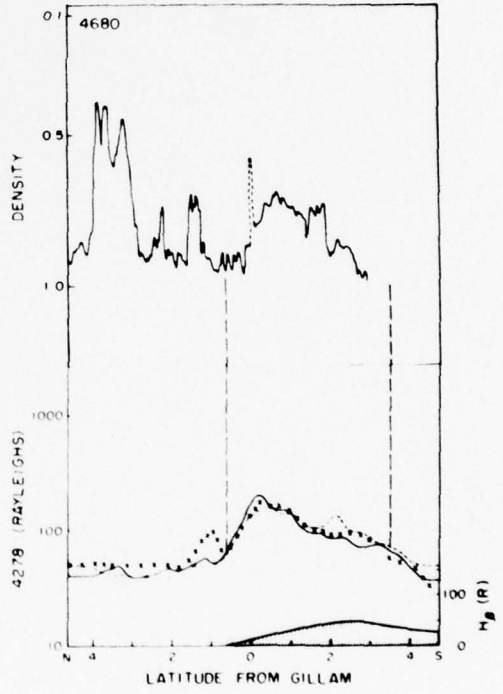
4680
DENSITY
4278 (RAYLEIGHS)
LATITUDE FROM GILLAM

Fig 6a b c


2/18/75
0614 UT
ORBIT4807
2/13/75
0747 UT
ORBIT4737
2/08/75
0739 UT
ORBIT4666

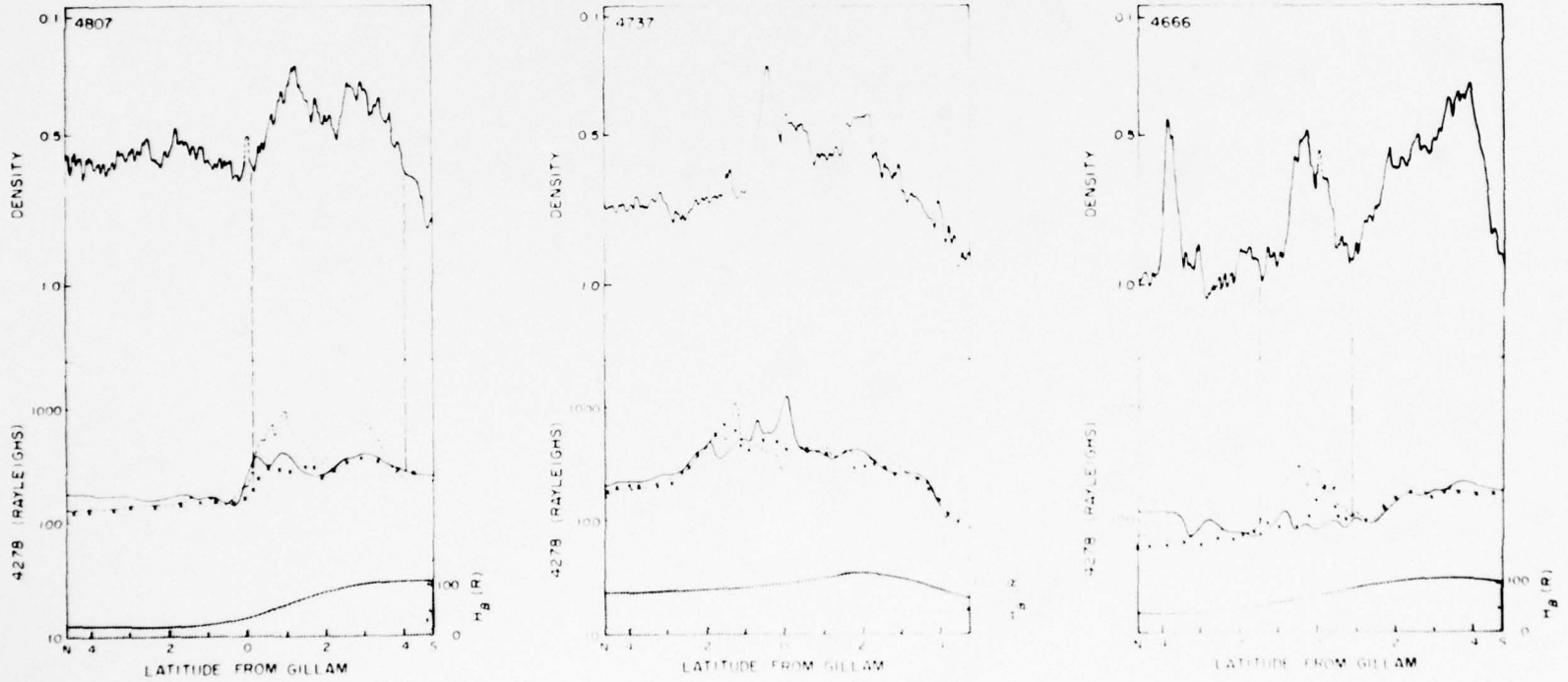
4807
4737
4666
DENSITY
4278 (RAYLEIGHS)
LATITUDE FROM GILLAM

Fig. 7a,b,c.


2/17/75
0632 UT
ORBIT4793
3/05/75
0820 UT
ORBIT5021
2/08/75
0557 UT
ORBIT4665

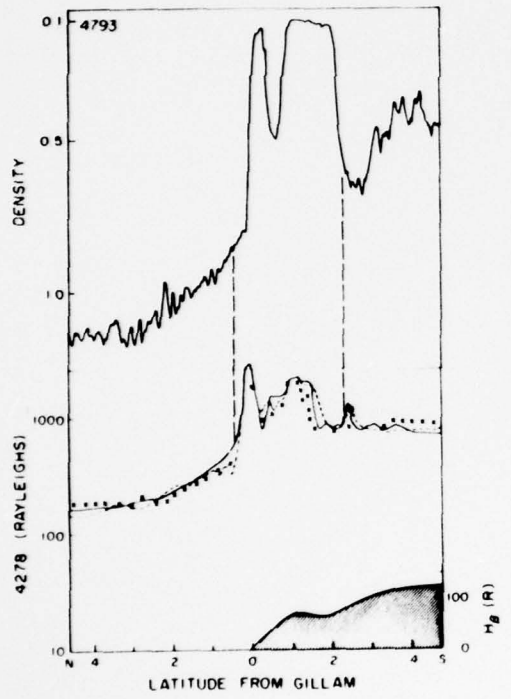
4793
DENSITY
4278 (RAYLEIGHS)
H_β (R)
LATITUDE FROM GILLAM

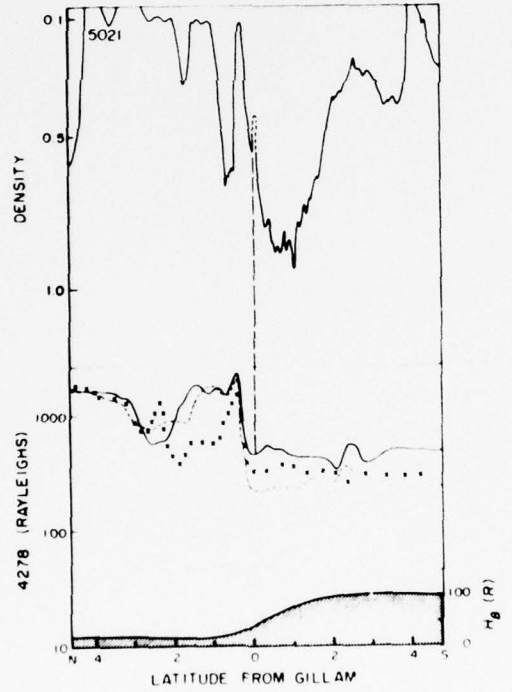
5021
DENSITY
4278 (RAYLEIGHS)
H_β (R)
LATITUDE FROM GILLAM

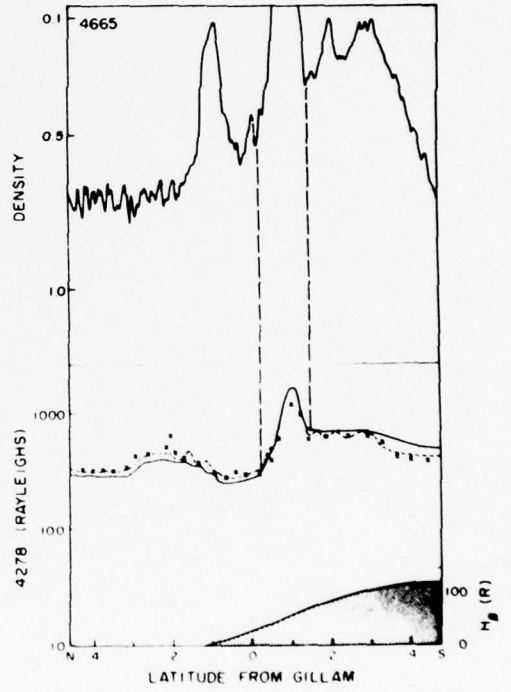
4665
DENSITY
4278 (RAYLEIGHS)
H_β (R)
LATITUDE FROM GILLAM

Fig. 8a,b,c.

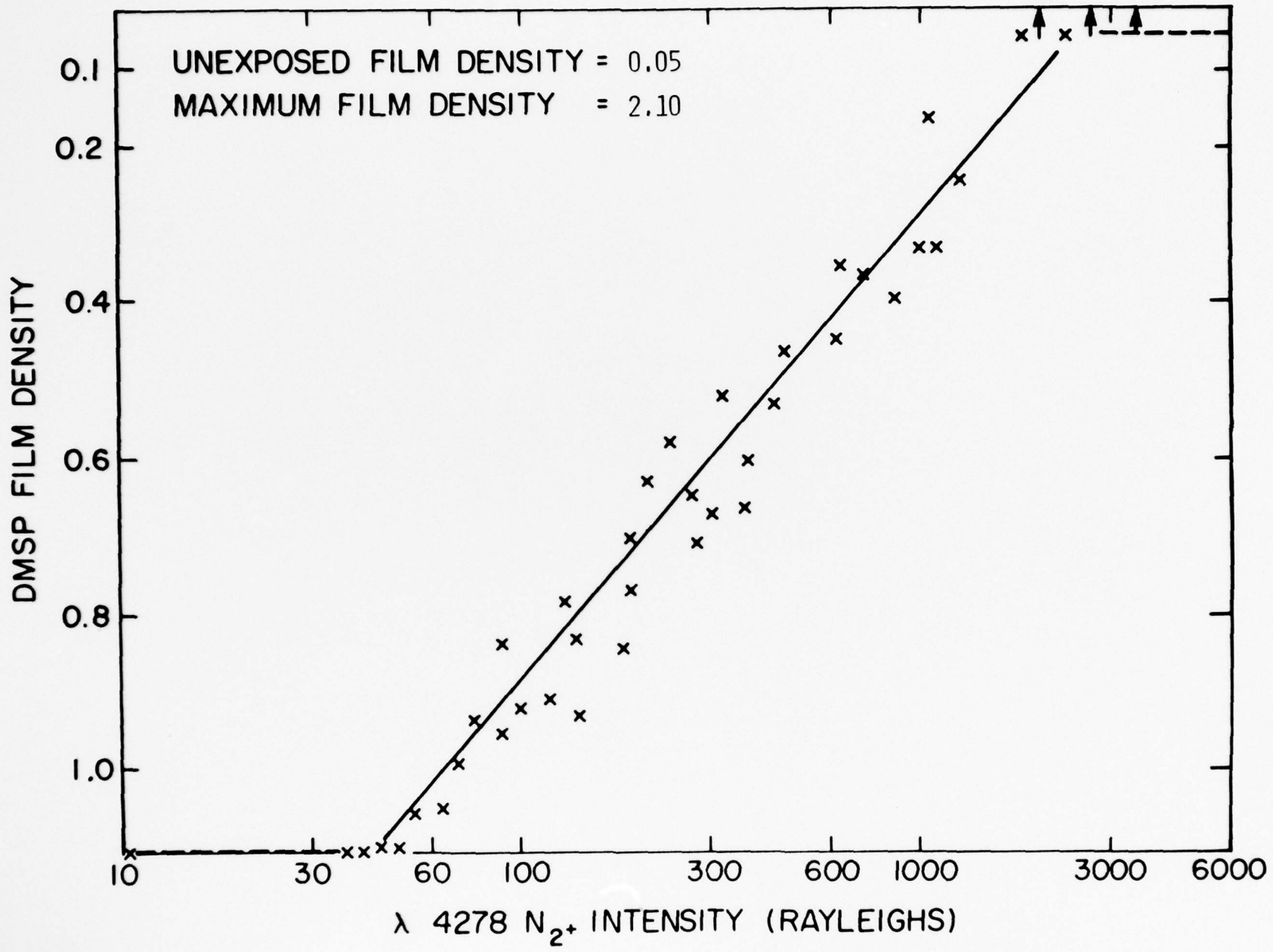
UNEXPOSED FILM DENSITY = 0.05
MAXIMUM FILM DENSITY = 2.10
DMSP FILM DENSITY
0.1
0.2
0.4
0.6
0.8
1.0
10
30
60
100
300
600
1000
3000
6000
λ 4278 N2+ INTENSITY (RAYLEIGHS)

Figure 9


3/13/75 0734 UT
ORBIT 5134

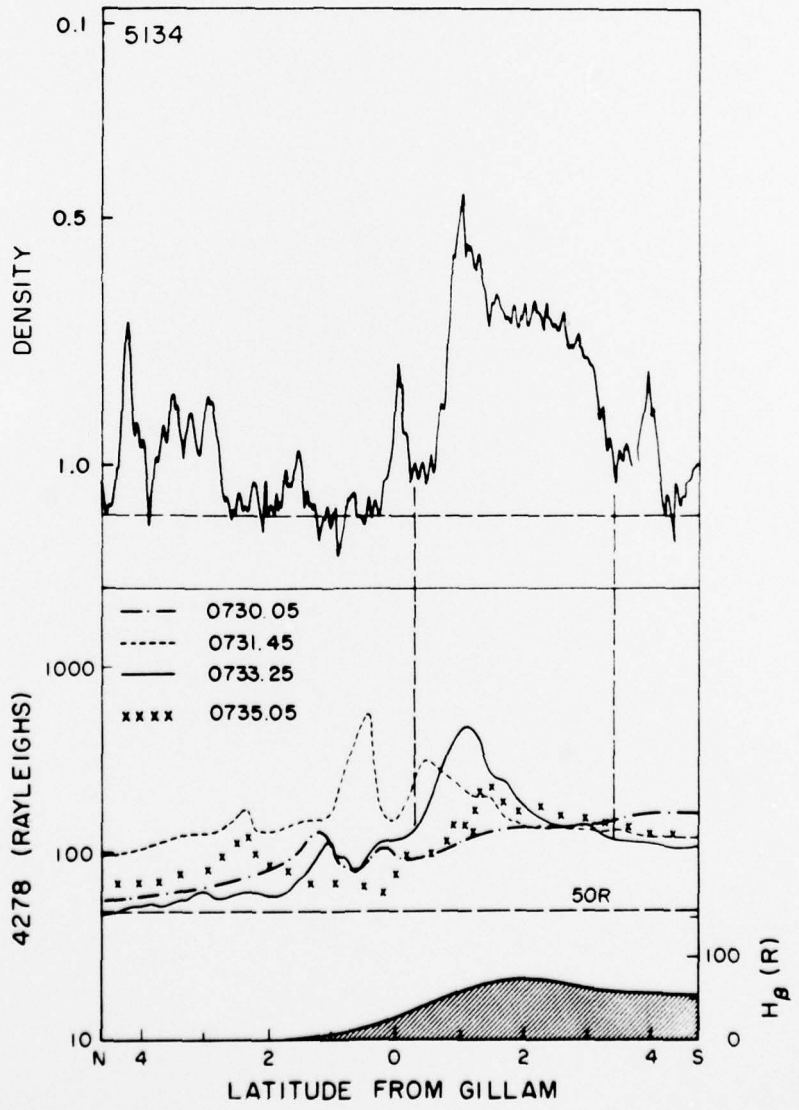
5134
DENSITY
0.1
0.5
1.0
0730.05
0731.45
0733.25
0735.05
4278 (RAYLEIGHS)
1000
100
10
50R
100
0
H_β (R)
N 4 2 0 2 4 S
LATITUDE FROM GILLAM

Figure 10.

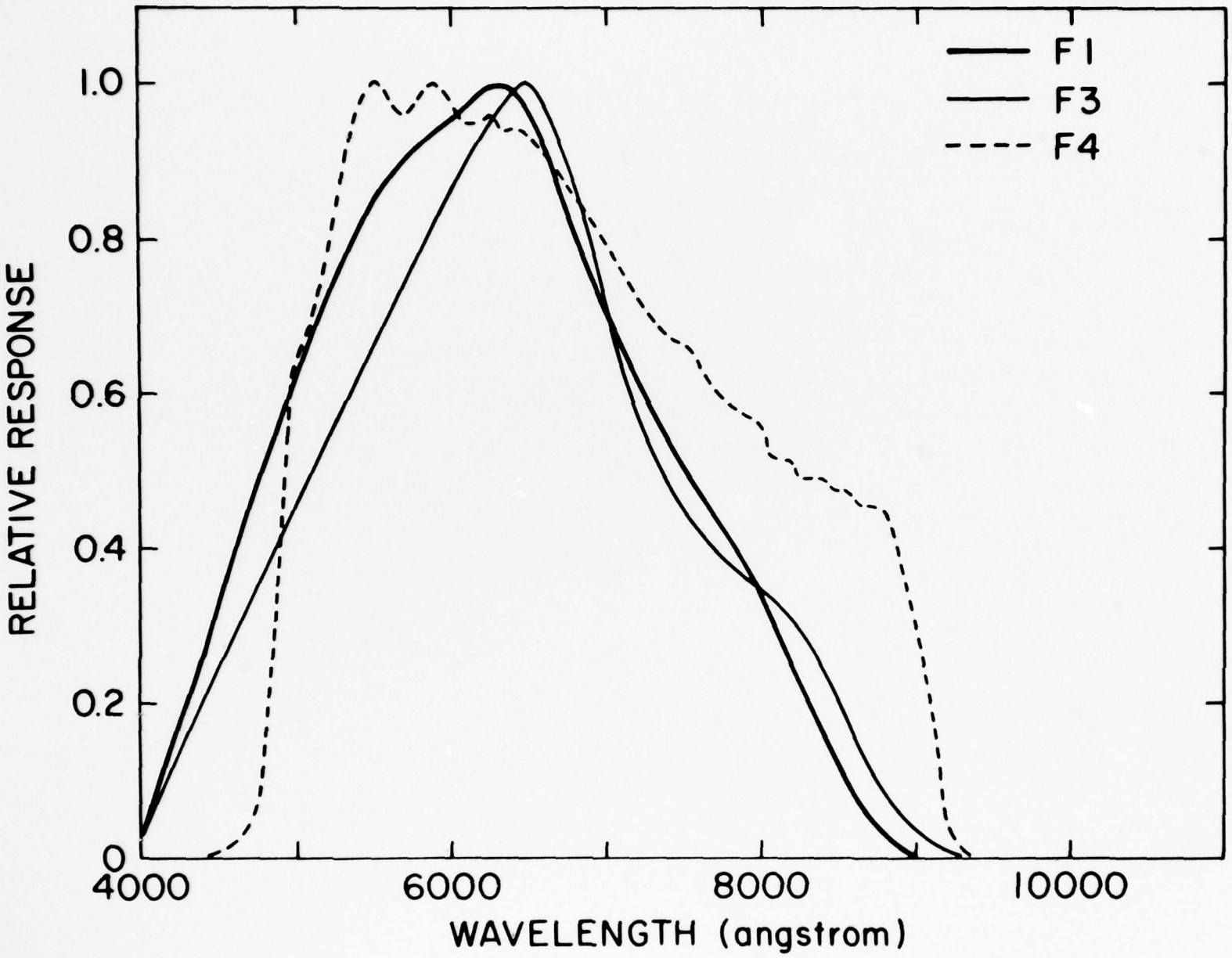
F1
F3
F4
RELATIVE RESPONSE
1.0
0.8
0.6
0.4
0.2
0
4000
6000
8000
10000
WAVELENGTH (angstrom)

Fig. 11a

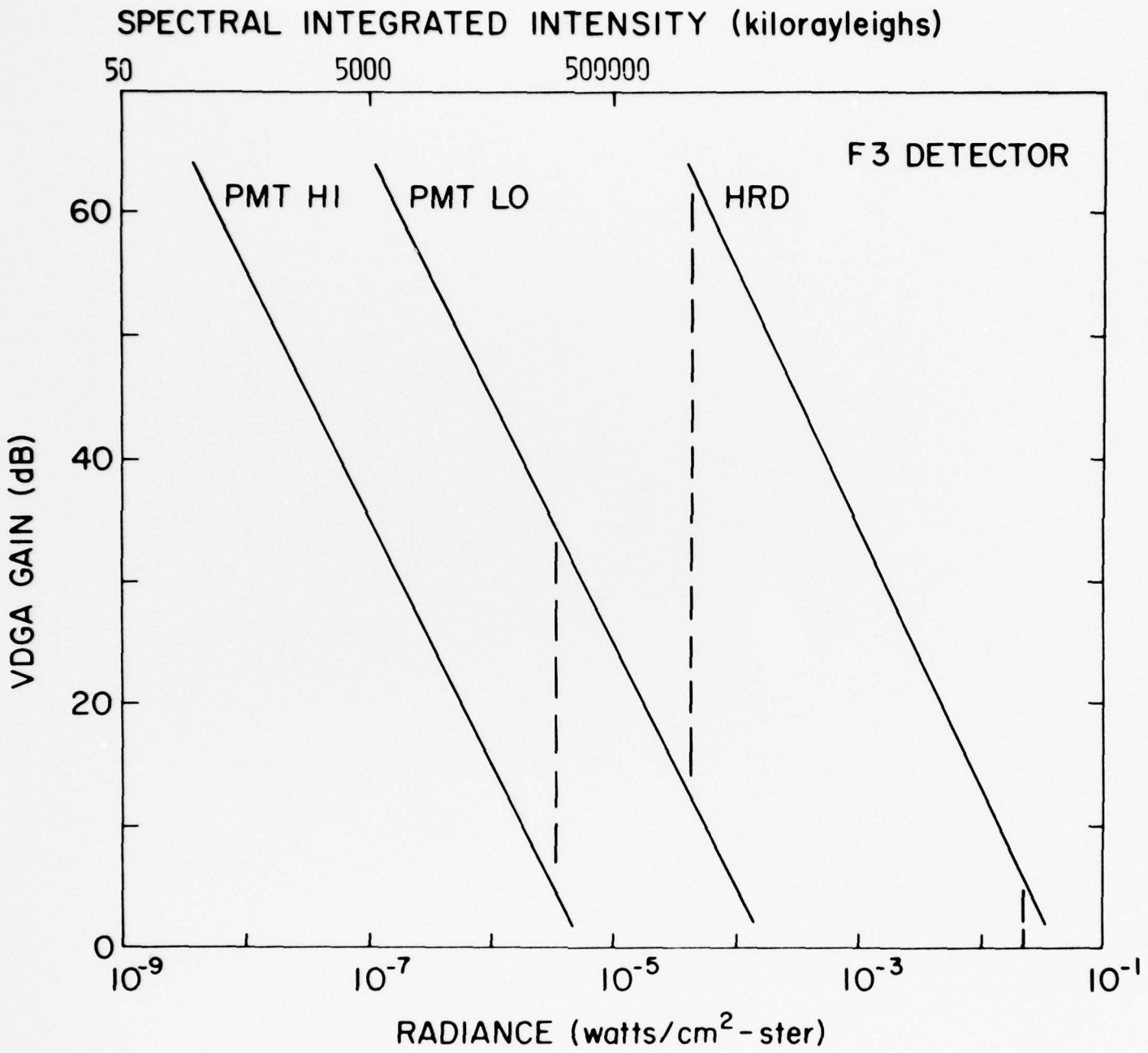
SPECTRAL INTEGRATED INTENSITY (kilorayleighs)
50
5000
500000
F3 DETECTOR
PMT HI
PMT LO
HRD
60
40
20
0
VDGA GAIN (dB)
10^{-9}
10^{-7}
10^{-5}
10^{-3}
10^{-1}
RADIANCE (watts/cm^2-ster)

Fig. 11b

ORIGINAL 8" POSITIVE, EMULSION SIDE UP

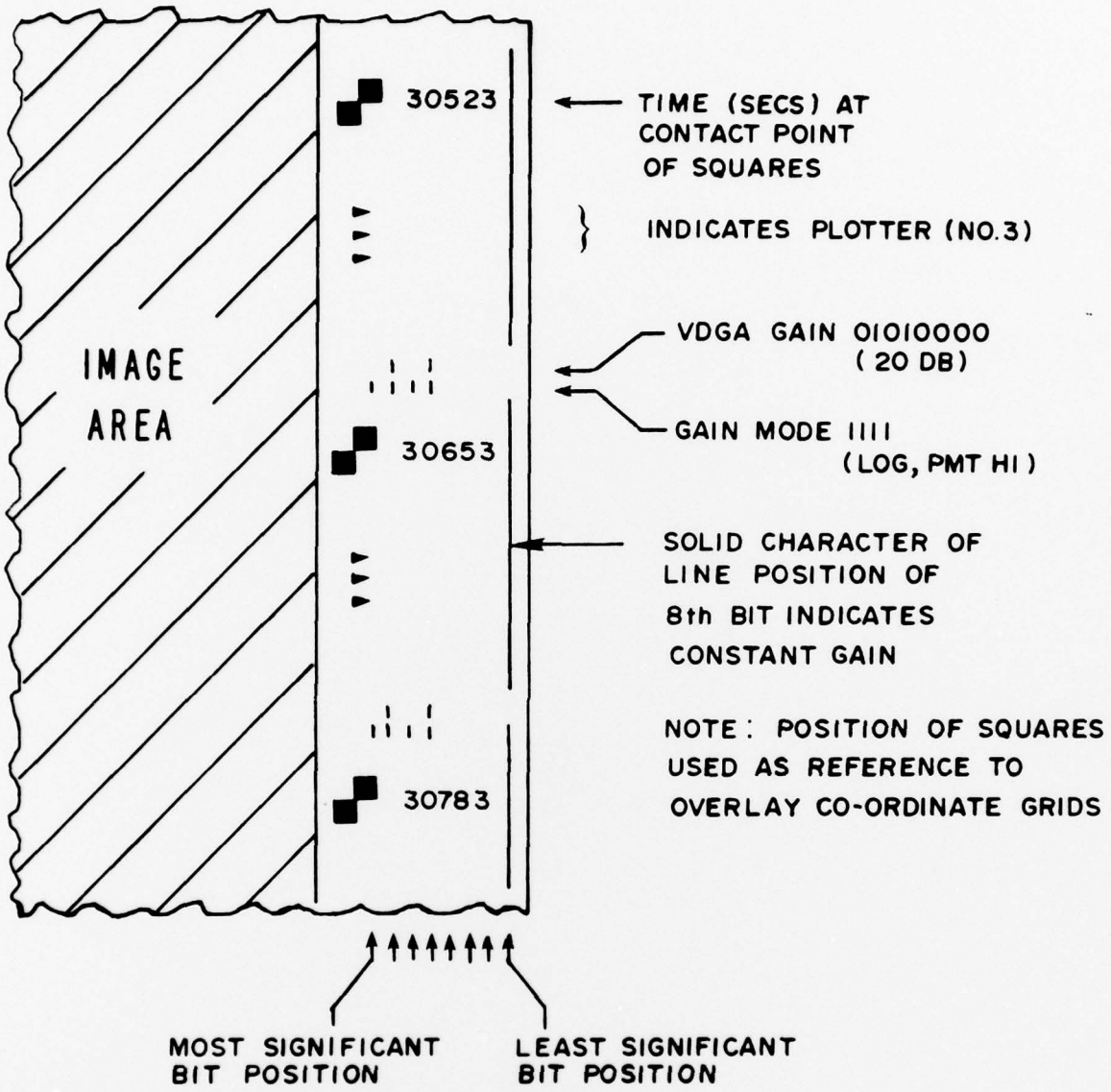

VDGA BIT NUMBER	1	2	3	4	5	6	7	8
DB	32	16	8	4	2	1	1/2	1/4

GAIN MODE CODE: (FOR AURORAL SITUATIONS)		
1 0 1 1	LOG, PMT 1/9
0 0 1 1	LIN, PMT 1/9
1 1 0 1	LOG, PMT LO
0 1 0 1	LIN, PMT LO
1 1 1 1	LOG, PMT HI
0 1 1 1	LIN, PMT HI

Figure 12

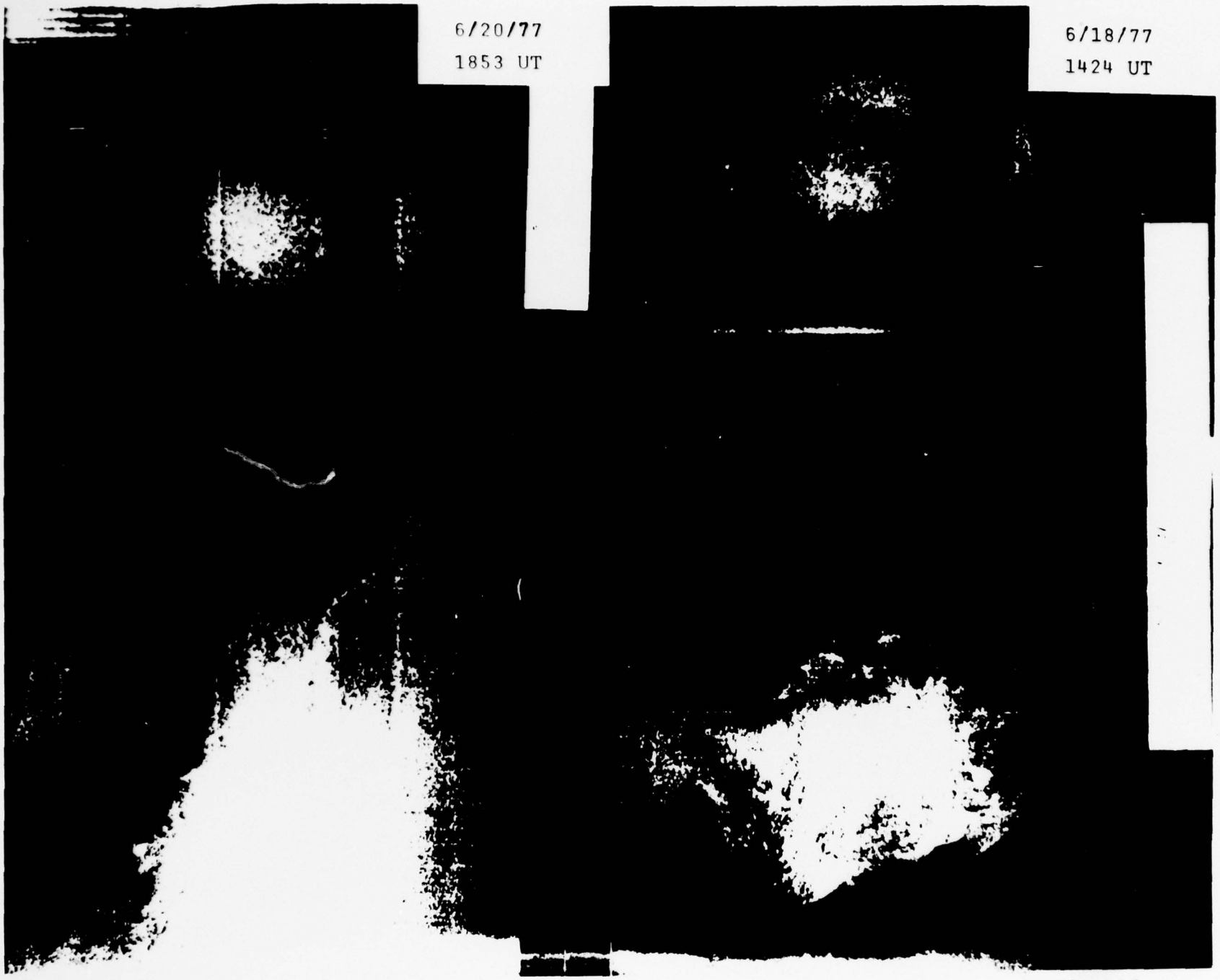

AFGL PHOTO 58-918

Fig. 13

UNCLASSIFIED

SECURITY CLASSIFICATION OF THIS PAGE (When Data Entered)

REPORT DOCUMENTATION PAGE	READ INSTRUCTIONS BEFORE COMPLETING FORM
1. REPORT NUMBER: AFOSR-TR- 78-1501 / 2. GOVT ACCESSION NO.	3. RECIPIENT'S CATALOG NUMBER
4. TITLE (and Subtitle): CO-ORDINATED ANALYSIS OF AURORAL DATA ON THE ATS FIELD LINE	5. TYPE OF REPORT & PERIOD COVERED: Final Report 06/30/76 - 03/31/78
	6. PERFORMING ORG. REPORT NUMBER
7. AUTHOR(s): Robert H. Eather	8. CONTRACT OR GRANT NUMBER(s): F44620-76-C-0129
9. PERFORMING ORGANIZATION NAME AND ADDRESS: Boston College, Chestnut Hill, MA 02167	10. PROGRAM ELEMENT, PROJECT, TASK AREA & WORK UNIT NUMBERS: 2311/A1 61102F
11. CONTROLLING OFFICE NAME AND ADDRESS: Air Force Office of Scientific Research/NP, Bldg. 410, Bolling AFB, D.C. 20332	12. REPORT DATE: August 31, 1978
	13. NUMBER OF PAGES
14. MONITORING AGENCY NAME & ADDRESS (if different from Controlling Office)	15. SECURITY CLASS. (of this report): Unclassified
	15a. DECLASSIFICATION DOWNGRADING SCHEDULE

16. DISTRIBUTION STATEMENT (of this Report)

Approved for public release - distribution unlimited.

17. DISTRIBUTION STATEMENT (of the abstract entered in Block 20, if different from Report)

18. SUPPLEMENTARY NOTES

19. KEY WORDS (Continue on reverse side if necessary and identify by block number)

Aurora

DMSP calibration

20. ABSTRACT (Continue on reverse side if necessary and identify by block number)

This report describes data analysis of meridian-scanning photometer data and satellite particle data, taken on the ATS field line. The particles that generate diffuse aurora are identified. A complete absolute calibration of the DMSP imaging system is presented. Ongoing co-ordinated analysis is described.

DD FORM 1 JAN 73 1473 EDITION OF 1 NOV 65 IS OBSOLETE